AMORPHOUS LACTOSE CRYSTALLISATION KINETICS

A thesis presented in partial fulfilment of the requirements for the degree
of Master of Engineering
in
Bioprocess Engineering

at Massey University, Manawatu,

New Zealand.

Zachary Clark

2012

Abstract

The crystallisation kinetics of amorphous lactose were investigated at different relative humidity and temperature combinations. Relative humidity was controlled by placing the amorphous lactose in sealed pans containing saturated salt solutions. These pans were stored, for defined time periods, at temperatures ranging from 10-40°C above the glass transition temperature (T_g). The degree to which crystallisation had occurred was measured using both dynamic vapour sorption and isothermal microcalorimetry. The results showed crystallisation to be an all or nothing event, such that a direct measurement of the kinetics could not be obtained. This is not well accounted for by Avrami type models. It is proposed that the rapid crystallisation could be an autocatalytic effect as moisture is released during crystallisation, or a showering event as is seen in highly supersaturated lactose solutions. The latter is supported by the observation that experiments using Supertab (a blend of crystalline and amorphous lactose) show crystallisation at lower T_g conditions than is required for the crystallisation of 100% amorphous lactose.

As part of confirming the equilibrium time for amorphous lactose particles the diffusion rates were investigated. The diffusivity of water through lactose was estimated by fitting a model to the DVS results. Diffusivities of $3.4 \cdot 10^{-13}$, $1.4 \cdot 10^{-14}$, $7.6 \cdot 10^{-12}$ and $3.6 \cdot 10^{-13}$ m^2s^{-1} were found for Supertab, spray dried, freeze dried and milled lactose, respectively.

Acknowledgments

Special thanks to my primary supervisor, Tony Paterson, for his help and support. I was fortunate to have him as a supervisor. Thanks also to Raymond Joe at Fonterra, for his help and use of the lab. Also, Tony Styles for his backing. Thanks to Jeremy Mcleod at Hilmar as well, for his insights and support. I appreciate everyone's time and efforts for the meetings and jobs dealt with due to the project.

Previous research, mainly by Tony Paterson, John Bronlund and Georg Ripberger, was also very helpful.

The project was funded with the support of Fonterra NZ and Hilmar Cheese. I am grateful to both companies for doing so.

Table of Contents

List of Figures

1 Introduction

Lactose is typically derived from the permeate produced during the ultrafiltration of whey or milk. The process of lactose manufacture includes concentration, crystallisation, washing and drying. The drying step involves using a heated air stream to flash off the moisture remaining after the crystals have been separated, using a centrifuge, from the wash water. During the drying step, if the removal of moisture is rapid enough that the lactose molecules remaining dissolved in the residual moisture are unable to be incorporated in the crystal structure, amorphous lactose is formed. This form of lactose is often undesired as it can cause stickiness and caking problems. As well as formation it is also probable that some crystallisation of the amorphous lactose occurs during the drying process. This is expected because it is known that where the glass transition temperature is exceeded, it becomes possible for lactose molecules in the amorphous state to become mobile and crystallised. These conditions exist in the fluidized bed drying process used in lactose manufacture. Whilst it is known that these conditions exist, the kinetics of amorphous lactose crystallisation under these conditions are not known, making it difficult to predict the impact any changes to drying conditions will have on amorphous lactose crystallisation. It is the aim of this work to improve the understanding of the kinetics at conditions similar to those found in a fluidised bed drier. It will aim to do so in reference to the conditions of the industrial drying process setup at industrial plants.

2 Literature Review

2.1 Lactose

Lactose is the main carbohydrate component of cow's milk, making up about 4.8% by weight (Kellam, 1998). It is a disaccharide made up of glucose and galactose with the molecular formula $C_{12}H_{22}O_{11}$. Both α and β forms exist, with the difference being the orientation of the hydroxyl group on the C-1 carbon of the glucose ring (Figure 2-1). In solution, the two forms are in equilibrium and can convert via mutarotation. At 20°C, lactose exists in an equilibrium, with 62.7% β-lactose and 37.3% α-lactose (Roetman & Buma, 1974).

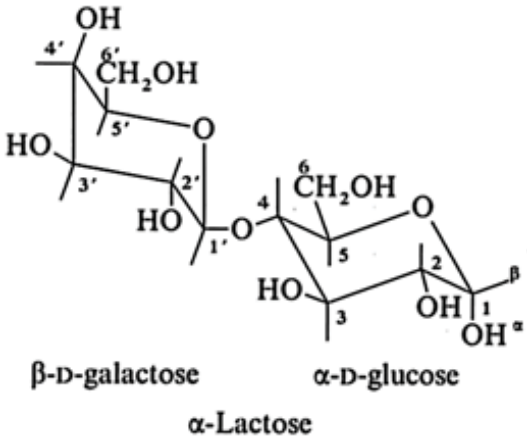

Figure 2-1:α-Lactose Structure (Roelfsema, Kuster, Heslinga, Pluim, & Verhage, 2000).

A summary of the physical differences between the anomers is given below in Table 1.

Table 1: Physical properties of both lactose anomers (Harper, 1992; Kellam, 1998)

	Units	α-lactose monohydrate	β-lactose anhydride
Molecular weight	g/mol	360.3	342.3
Melting point	°C	202	252
Density	g/ml	1.545	1.59
Specific optical rotation	α^{20}_{589}	+91.55	+33.5
Heat of solution	J/g	-50.2	-9.6
Solubility in water (20°C)	g/100 ml	7.4	50.00

2.2 Lactose Production

Lactose is produced through crystallisation. As well as being a valuable product, lactose has a high BOD, so removing it from waste streams by crystallisation is desirable. The raw product for edible grade lactose production is whey or whey permeate. This is concentrated, then cooled allowing crystals to form. The crystals are then separated from the mother liquor, washed and dried, prior to packing. The drying step typically involves a flash drier followed by a fluidized bed drier (McLeod, 2007). The process flow diagram for the manufacturing process is shown below in Figure 2-2. During the flashing off of water a small layer of amorphous lactose is formed on the surface of the crystals (Paterson, 2009). The layer of amorphous lactose is presumed to crystallise in the fluidised bed drier that follows. Fluidised bed dryers are characterised by high heat and mass transfer rates and low residence times.

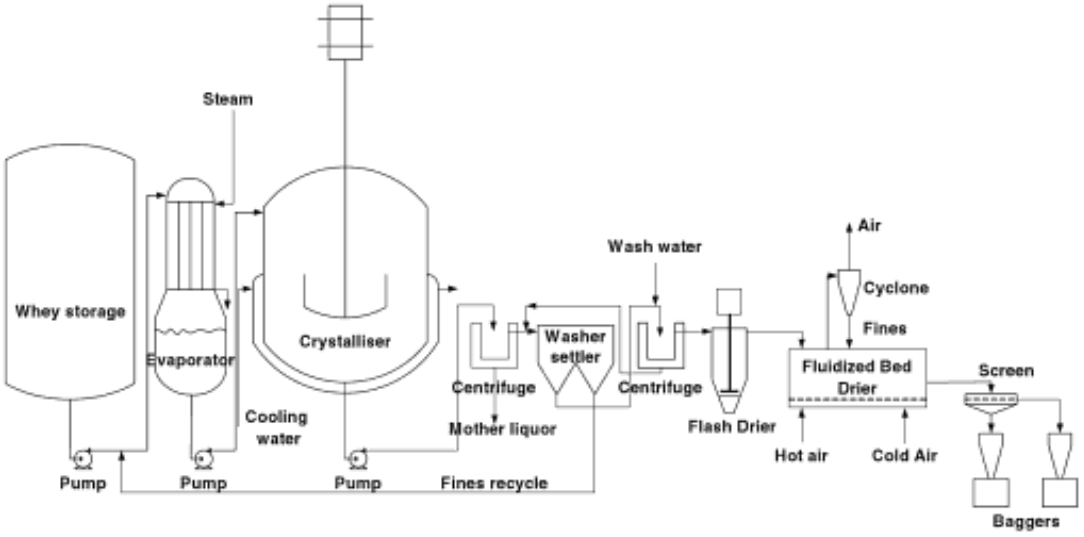

Figure 2-2:Process flow diagram for manufacture of edible grade α-lactose monohydrate (Paterson, 2009).

To produce pharmaceutical grade lactose further refinement is required. A combination of adsorption and filtration processes are required to remove impurities such as riboflavin, a variety of proteins, lactose phosphate and lactic acid, before the solution is pumped to the evaporator (Paterson, 2009).

2.3 Lactose Forms

2.3.1 Crystalline Lactose

The molecules in crystalline lactose are highly ordered. There are four well accepted forms of lactose, three of which are anhydrous and one hydrated (Kirk, Dann, & Blatchford, 2007). The most common commercially produced form is α-lactose monohydrate. There is also: stable anhydrous α lactose, unstable (hygroscopic) anhydrous α lactose and β-lactose anhydride. The hydrated form, α-lactose monohydrate, is formed by crystallisation of lactose solution below 93.5°C. Above 93.5°C β-lactose anhydrate forms (a_w = 0.58; (Vuataz, 1988)). A mix of α and β lactose can also crystallise (Miao & Roos, 2005).

2.3.2 Amorphous Lactose

In amorphous lactose the molecules are randomly distributed. It lacks the long-range translational symmetry that defines a crystalline structure. Due to its tendency to induce caking, which can cause storage and handling problems, it is often an undesired product (Aguilera, del Valle, & Karel, 1995). It is usually a mixture of α-lactose, β-lactose and water (0-10%). It forms when rapid drying of the lactose solution causes a rapid viscosity increase that prevents crystallisation.

2.3.3 Partially Amorphous Lactose

A layer of amorphous lactose can be formed during spray drying of a lactose crystal solution, freeze drying and through melting and rapid cooling (milling) (Che & Chen, 2010). A 100 g sample of commercial spray dried lactose was found to contain: α-monohydrate (81.7 g), α-anhydrous (2.6 g), β-anhydrous (10.8 g), amorphous α-lactose (2.2 g) and amorphous β-lactose (2.7 g) (Che & Chen, 2010). Figure 2-3 shows both the amorphous and crystalline forms within the same material.

Supertab is a form of partially amorphous lactose manufactured for DMV-Fonterra Excipients. It is produced by spray drying and contains 5-12% amorphous lactose. Due to Supertab's high flowability, even when exposed to conditions under which amorphous lactose would typically become sticky, it is likely the amorphous regions are located near the centre of the lactose particle.

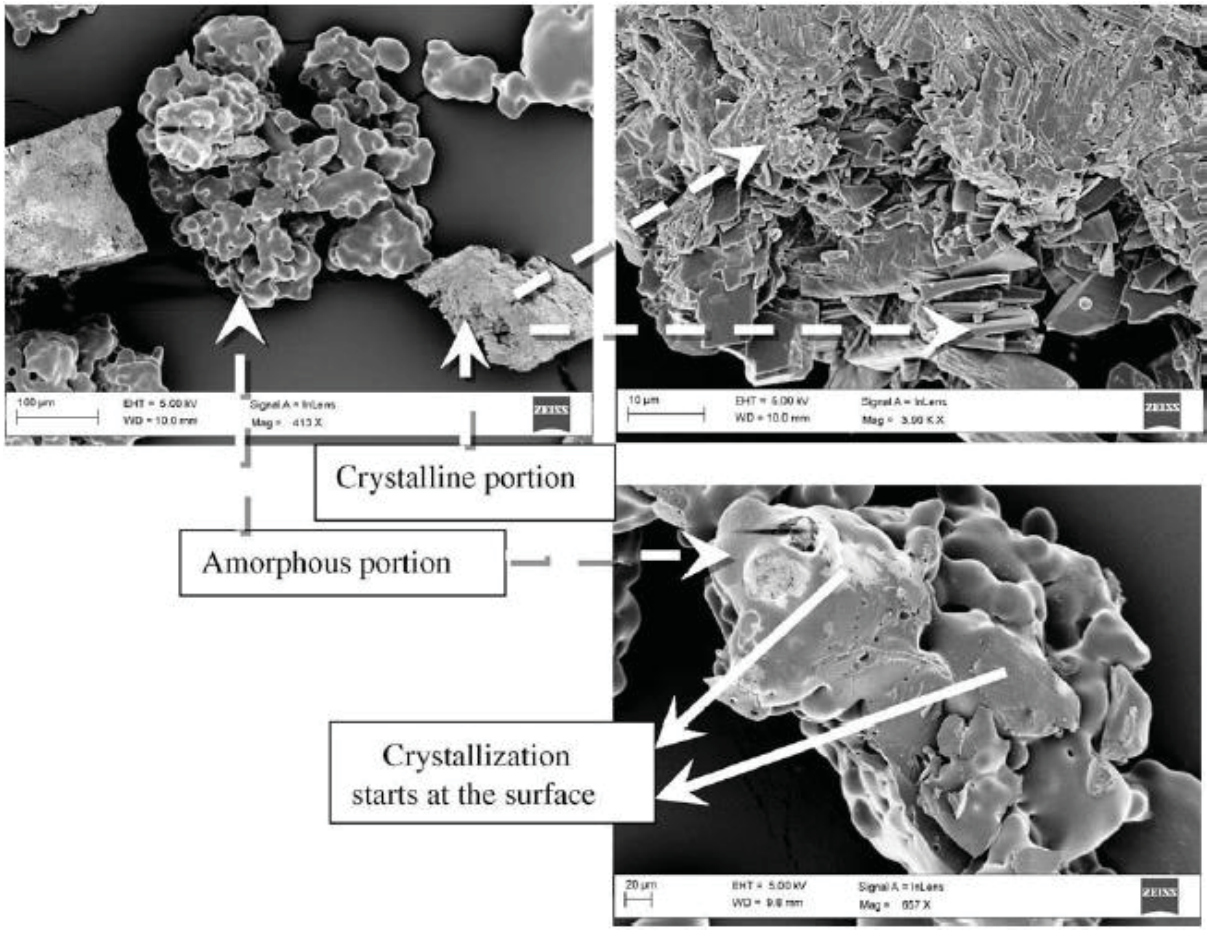

Figure 2-3: Micrograph of spray dried lactose (220°C gas inlet) containing both amorphous and crystalline regions (Whiteside et al., 2008).

2.4 Glass Transition Temperature

The temperature at which an amorphous material changes physical state is known as the glass transition temperature (T_g). T_g has been called the most important characteristic of amorphous systems (Lin & Chen, 2002). Above T_g, viscosity decreases and the amorphous material changes from a solid glass-like form to a more liquid form. This allows molecules to flow, collapse and crystallise (Downton, Flores-Luna, & King, 1982). Water acts as a plasticiser reducing T_g (Levine & Slade, 1986; Roos & Karel, 1991; Thomsen, Jespersen, Sjostrom, Risbo, & Skibsted, 2005).

2.5 Amorphous Lactose

Amorphous lactose is hygroscopic; it has a high absorption capacity. It can contain 100 times more free moisture than the crystalline form (Bronlund & Paterson, 2004). When amorphous lactose crystallises it releases much of this water.

Molecular mobility is the main factor that determines the formation of amorphous systems (Palzer, 2010). Around the glass transition temperature (T_g) molecule clusters are released that

can rotate and slip past each other. The system changes from glassy to rubbery. The glass transition is a non-isothermal process with physical changes occurring slowly as temperature increases.

As Figure 2-4 shows, for amorphous structures, the free volume steadily increases as temperature increases until T_g, where the change in free volume increases significantly. In contrast, when heating crystalline structures there is a discontinuous change at the melting temperature (T_m).

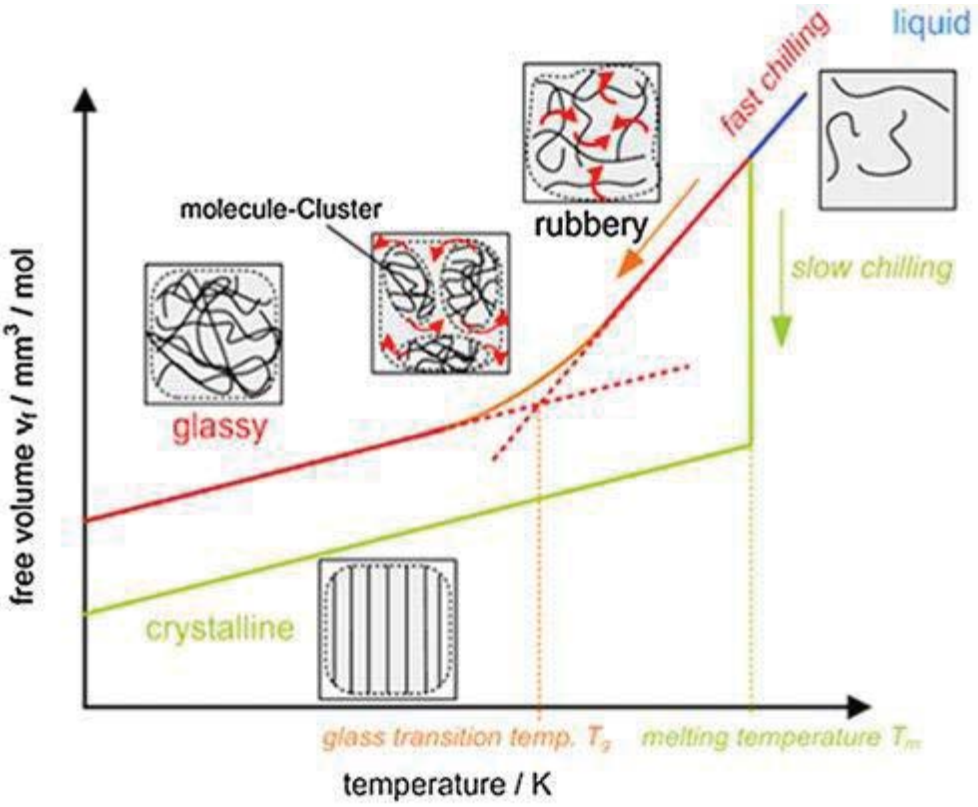

Figure 2-4:Free specific volume in crystalline and amorphous structures against temperature (Palzer, 2010).

2.5.1 Diffusivity of lactose types

A model of moisture sorption onto a monolayer of lactose for spray dried and freeze dried produced amorphous lactose was constructed by Ripberger (2010). Spray dried lactose took about twelve hours to reach equilibrium. When results were adjusted for agglomerates there was a significant difference between the diffusivities of the 10% and 30% lactose spray dried solutions. Ripberger found values of $3.41 \cdot 10^{-14}$, $6.59 \cdot 10^{-14}$ and $4.48 \cdot 10^{-11}$ m^2s^{-1} for the diffusivity of spray dried (30% and 10% lactose solutions) and freeze dried lactose (20%) respectively. The significant difference between the diffusivity of water through spray and

freeze dried lactose is partly because the spray dried particles shrink during production. As drying occurs above T_g molecular mobility is high, encouraging lactose-lactose interactions and resulting in a dense matrix (Vollenbroek, Hebbink, Ziffels, & Steckel, 2010; Vuataz, 2002). In contrast, as well as not shrinking, the freeze dried lactose particle is formed at low temperatures and low molecular mobility. Thus, there was a higher free volume and better adsorption conditions for the freeze dried lactose. Moisture isotherms experiments have confirmed that freeze dried lactose has more open sites for water to absorb at low relative humidities (Vollenbroek et al., 2010). Conditioning samples by holding them slightly above the glass transition allows relaxation of molecules to take place, and the differences in moisture sorption are reduced.

2.5.2 Sticking & Caking

Sticking and caking are terms used to describe powder cohesion. Caking is often described as the change of amorphous powders into lumps and then a clumped solid (Paterson, Brooks, Foster, & Bronlund, 2005). Caking is a two-step process; first the particles must bridge together (sticking), and then solidify. The extent of stickiness determines the extent of caking in the powder (Paterson et al., 2005).

Amorphous lactose is known to cause sticking. Amorphous lactose becomes rubbery at temperatures above T_g, increasing the rate of sticking and caking (Bhandari & Howes, 1999; Lloyd, Chen, & Hargreaves, 1996). Bronlund (1997) suggested that liquid bridges can form between particles when T_g is exceeded. As water is absorbed from the environment this causes a reduction in viscosity and T_g, facilitating crystallisation. The plasticisation effect increases molecular mobility and allows a more stable crystalline structure to form (Burnett, Thielmann, Sokoloski, & Brum, 2006; Elmonsef Omar & Roos, 2007). Thus, the caking process is also responsible for stabilising the powder. Figure 2-5 illustrates the plasticisation effect of water and gives an approximate division between the unstable and stable zones for amorphous lactose.

To prevent caking in lactose powders with amorphous lactose Bronlund (1997) recommended storing it at humidities below 25%. Others recommend storing below 30% RH (Che & Chen, 2010).

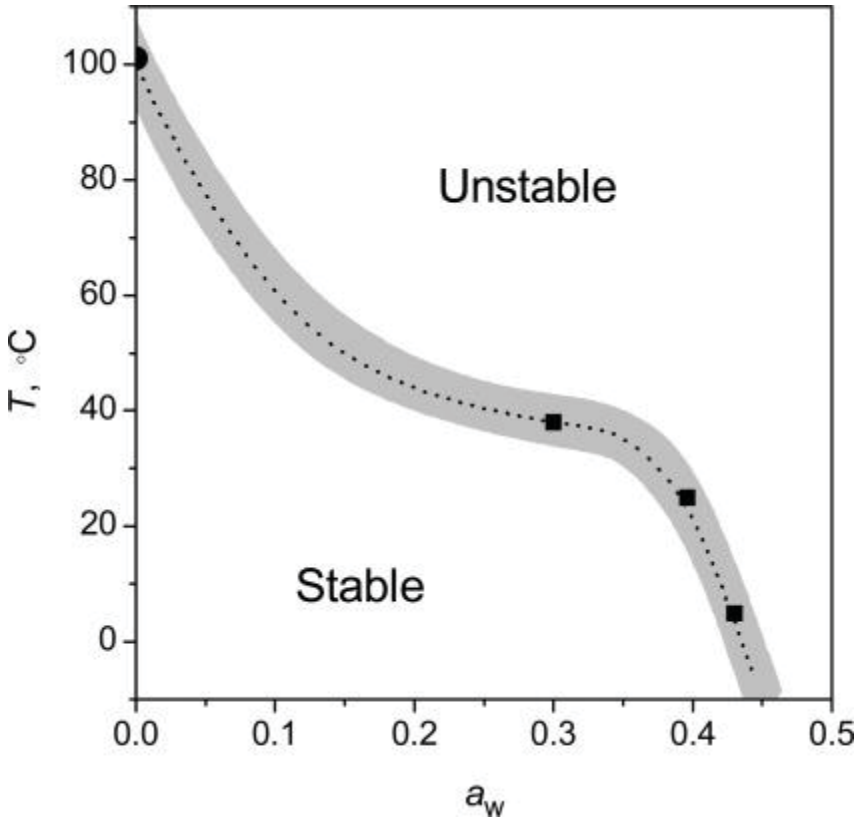

Figure 2-5: Water activity state diagram for amorphous lactose. Dotted line and transition zone drawn as guide only (Thomsen et al., 2005).

2.6 Moisture Isotherms for amorphous lactose

Water has a plasticising effect on amorphous lactose reducing T_g. This makes having an accurate measurement of the moisture content of amorphous lactose very important when investigating T_g and amorphous lactose crystallisation. Moisture sorption isotherms can be used to show the relation between moisture content and water activity at a certain temperature.

An important quantity in measuring moisture contents of foods is water activity (a_w). As stated in equation (1) water activity is the ratio of the vapour pressure of water in the substance over the vapour pressure of pure water. Water activity is equal to the relative humidity of the ambient air at equilibrium. It is used, in preference to moisture content, as it is both a more sensitive index, and is easier to measure. The two are interchangeable when the isotherm for the material is known.

$$a_w = \frac{p_w}{p_o} \quad (1)$$

The Guggenheim, Anderson, de Boar (GAB) isotherm model describing multilayer adsorption is stated in equation (2). Water content and the water required for a monomolecular layer of water molecules on the solid are w' and w'_m. The constants, C and K, are related to the energy of the different sorption layers. However, Bronlund (1997) argues that because the GAB model describes surface absorption rather than a diffusion controlled sorption process the physical meaning of the constants are invalid for amorphous lactose. In the special case of K = 1, the GAB equation reduces to the Brunauer, Emmet and Teller (BET) equation. The BET model treats each layer equally, unlike the GAB model that recognises differences in the interaction between layers. Thus, the BET model is only valid when the covering of the first layer dominates ($0.05 < a_w < 0.4$) (Vollenbroek et al., 2010).

$$\frac{w'}{w'_m} = \frac{C.K.a_w}{(1-K.a_w).(1+(C-1).K.a_w)} \quad (2)$$

Typically, amorphous lactose isotherms are only shown for a range of 0 to 0.6 as above this water activity crystallisation occurs at room temperature. The GAB model is shown to accurately predict moisture content for amorphous lactose over this range. The third stage sorption (TSS) model is an extension of the GAB model and is more accurate for high water activities that crystalline lactose may be exposed to (Timmermann & Chirife, 1991). Figure 2-6 below shows the moisture isotherm for amorphous lactose as well as the GAB model.

A plot comparing the sorption of freeze and spray dried lactose showed little difference between curves suggesting that the sorption behaviour of the two lactose types are very similar (Bronlund & Paterson, 2004; Brooks, 2000). However, at low relative humidity and amorphous levels there is a notable difference in the isotherms of spray and freeze dried lactose (Vollenbroek et al., 2010). Section 2.5.1 on diffusivity discusses this further.

The rate of moisture sorption is higher for crystalline lactose than amorphous lactose. This is because only surface adsorption is occurring in the crystalline case, for amorphous lactose water must adsorb onto the surface then also diffuse through the matrix (Ripberger, 2010).

Brooks (2000) showed that a correction should be applied to much of the literature sorption data gathered for predicting T_g. It was found that amorphous lactose dried over phosphorous pentoxide for extended periods still contained a small amount of residual water. A value of 1g/100g of dry powder was used for residual moisture to correct the literature data. A value of 115°C was given by Brooks as the corrected T_g at zero moisture content. Similar values were

found by Schmitt et al. (1999), 114°C, and Chen et al. (2001), 117°C. Haque & Roos (2004) found an onset temperature of 105.4°C and an end of 122.4°C for T_g using differential scanning calorimetry. A slight difference was found between the T_g of freeze dried and spray dried lactose suggesting that the different microstructures produced by these drying methods does effect crystallisation rate (Haque & Roos, 2006).

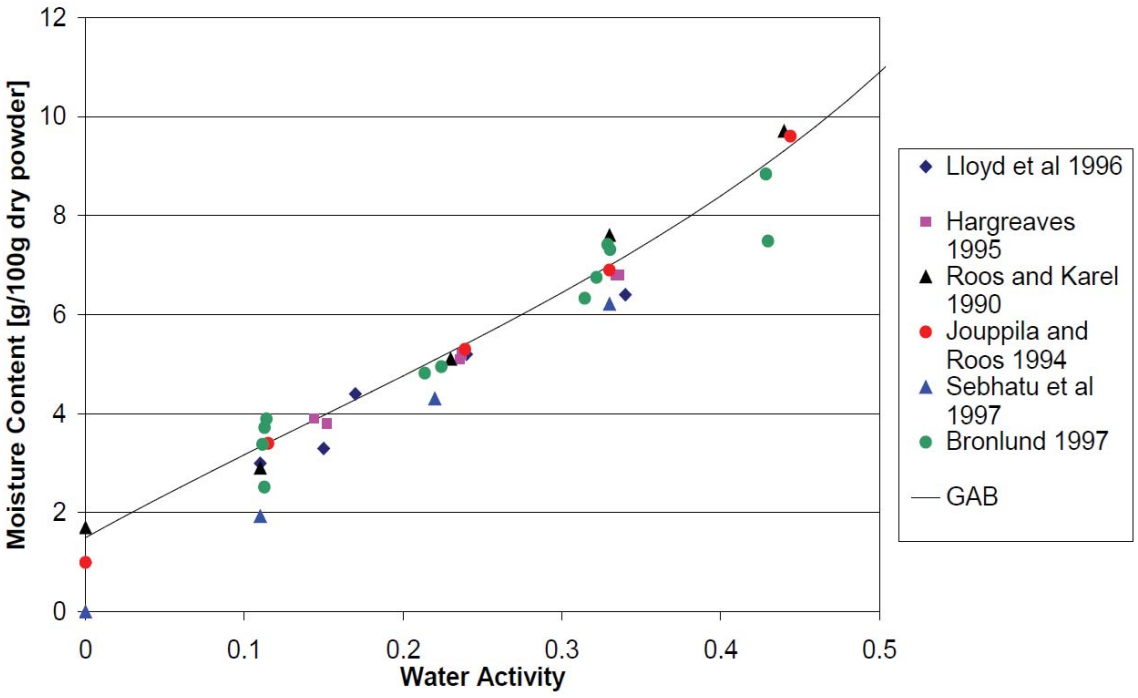

Figure 2-6: Amorphous lactose moisture isotherm (Foster 2000).

Brooks (2000) recommended the use of a cubic equation for prediction of T_g for a relative humidity less than 57.5%.

$$T_g = -530.66\,(a_w)^3 + 652.06\,(a_w)^2 - 366.33\,a_w + 99.458 \quad [0 < a_w < 0.575] \tag{3}$$

Bronlund and Paterson (2004) presented data from several sources and fitted the GAB model to show moisture sorption in amorphous lactose. They found that temperature has a negligible effect on the isotherm shape over the 20-40°C range.

The Gordon Taylor equation can also be used to predict T_g if the moisture content is known. It uses the mass fraction of water and solid substance ($w_w w_{so}$), the glass transition temperatures of water and solid ($T_{g,w} T_{g,so}$) and the constant, k'. Brooks (2000) found a value of 6.9 for k' (Gordon & Taylor, 1952).

$$T_g = \frac{w_w T_{g,w} + k' w_{so} T_{g,so}}{w_w + k' w_{so}} \quad (4)$$

2.7 Quantification of amorphous lactose

Table 2 shows a summary of the analytical techniques used to measure the degree of crystallinity of amorphous lactose. Obtaining the crystallisation kinetics involves measuring the amorphicity, moisture content, temperature and relative humidity.

2.7.1 X-ray Powder Diffraction (XRPD)

Crystalline materials diffract X-ray beams at distinct angles, producing clear peaks while amorphous materials produce more scattered peaks of variable intensity. With increasing amorphicity the peaks decrease and the baseline increases. A detection limit of 0.5% has been found for XRPD (Fix & Steffens, 2004).

2.7.2 Infra-Red (IR)

IR spectroscopy techniques are based on adsorption and use the spectral differences between amorphous and crystalline samples. The intensity of the vibrational bands is proportional to the phase concerned (Lin & Chen, 2002). Using calibrated samples various statistical techniques can be used to extract data from spectroscopic data. One can use multiple linear regression on the 2nd derivative spectra to determine the crystallinity of lactose powders (Nijdam, Ibach, & Kind, 2008). It has the capability to quantify amorphous contents as low as 1% (Hogan & Buckton, 2001).

2.7.3 Raman

Raman spectroscopy is based on light scattering and can measure the crystallinity of a single lactose particle. The radiation corresponding to vibrational energy transitions are measured. Fourier transform (FT) spectrometers and charge couple device (CCD) are often used as they avoid the interference due to fluorescence (Listiohadi, Hourigan, Sleigh, & Steele, 2008). Amorphous samples are characterised by a reduction in peak intensity and definition in the Raman spectra (Harjunen et al., 2004). Quantitative determination of amorphicity using Raman has found good agreement to XRPD (Lehto et al., 2006).

2.7.4 Solution Calorimetry

The enthalpy of solution ($\Delta_{sol}H$) or enthalpy associated with the addition of lactose sample into an over saturated lactose solution ($\Delta_{sat}H$) is measured. These can be correlated with the amorphicity of a sample.

2.7.5 Thermal Gravimetric Analysis (TGA)

TGA involves measuring the mass change of a sample to a change in temperature. TGA can be combined with single differential thermal analysis (SDTA) to allow the simultaneous measurement of both mass and energy. The area of under the exothermic crystallisation peak can be used to determine amorphous content with a detection limit of 1% estimated (Che & Chen, 2010).

2.7.6 Differential Scanning Calorimetry (DSC)

The amount of heat given out during crystallisation is proportional to the amorphicity of the sample. Use of a DSC involves holding a sample of amorphous lactose at a constant temperature above T_g, allowing it to crystallise exothermically, while measuring the difference in heating required between the sample and a reference. The reproducibility and accuracy of the results can be poor due to dehydration occurring during recrystallisation and overlapping of peaks (Lehto et al., 2006). However, if the change in specific heat capacity can be measured (modulated temperature DSC and hyper-DSC) the detection limit can be close to 1% or less. This is more difficult and requires modulated temperature DSC (MTDSC) or hyper DSC. StepScan DSC is another method that allows easier data interpretation, separating the glass transition from other events (Lin & Chen, 2006).

2.7.7 Isothermal Microcalorimetry (IMC)

In this approach a similar principle to DSC is used, in that the heat given out during crystallisation is measured. The sample is sealed in a glass ampoule with a saturated salt solution. Then the sample is held at a constant temperature and the power required as a function of time is measured. By controlling the humidity to a level that above T_g the amorphous fraction can be crystallised. Samples below 1% in amorphicity have been detected with this method (Lehto et al., 2006). Difficulties can arise due to variations in compositions of the starting material and salt solutions.

One instrument used in IMC is the Thermal Activity Monitor (TAM). It relies on the fact that the heat of crystallisation is proportional to the amorphicity of the sample. Integration of the heat flow peak gives an estimate of the heat of crystallisation. Samples below 1% in amorphicity have been detected with this method (Lehto et al., 2006). Billings (2002) found a detectable limit of 0.1% for amorphous sucrose.

Table 2: Comparison of quantification methods of amorphous lactose

	XRPD	NMR	NIRS	FT-Raman	SC	TGA/ SDTA	DSC	SS-DSC	Hyper-DSC	IMC	IGC	DVS	Isotherm
Approximate detection Limit	0.5%	< 0.5%	< 1%	1%	1%	1%	1-20%	< 1%	< 1.5%	< 0.5%	< 1%	0.7%	0.1%
					1.8%				< 1%	0.1% *			
Analysis time (hr)	< 1	0.5-10	< 0.5	0.1-2	< 1	< 1	< 1	< 1	< 0.5	0.5-4	5-13	1-5	3
Destructive	Yes	No	No	No	Yes	Yes	Yes	Yes	Yes	Yes	Yes	Yes	Yes
Sample weight (mg)	400	500-700	50	2000	200	5-15	3.5-4	1.6	1-3	20-300	500-1000	150	1000
			2000		400						50	50	800-1200
Reproducibility	Good	Good	Good	Good	Good	Good	Variable	Good	Good	Good	Good	Good	Good
Provides structural information	Yes	Yes	Possible	No	No	No	No	No	No	No	No	No	No
Crystallisation Kinetics (Yu, 2001)	Yes						Yes			Yes		Yes	Yes
References	(Fix & Steffens, 2004; Shah, Kakumanu, & Bansal, 2006)	(Gustafsson, Lennholm, Iversen, & Nyström, 1998)	(Fix & Steffens, 2004; Hogan & Buckton, 2001)	(Lehto et al., 2006; Shah et al., 2006; Whiteside et al., 2008)	(Harjunen et al., 2004; Hogan & Buckton, 2000)	(Listiohadi, Hourigan, Sleigh, & Steele, 2009)	(Fix & Steffens, 2004; Gombás, Szabó-Révész, Kata, Regdon Jr, & Eros, 2002)	(Lehto et al., 2006)	(Gabbott, Clarke, Mann, Royall, & Shergill, 2003; Saunders, Podluii, Shergill, Buckton, & Royall, 2004)	(Billings, 2002; Figura & Epple, 1995)	(Newell, Buckton, Butler, Thielmann, & Williams, 2001)	(Hogan & Buckton, 2001; Vollenbroek et al., 2010)	(Bronlund, 1997; Vollenbroek et al., 2010)

* Amorphous sucrose (Billings, 2002)

2.7.8 Gravimetric Methods

Due to the high adsorptive capacity of amorphous lactose compared with crystalline lactose gravimetric techniques are possible. Crystallisation is moisture induced, with desorption following. The amorphicity can be calculated, from the mass increase or decrease (Lehto et al., 2006; Vollenbroek et al., 2010).

Dynamic vapour sorption (DVS) is a common gravimetric method that involves controlling humidity using dry and wet gas streams (Burnett et al., 2006; Mackin et al., 2002). As Figure 2-7 shows, a step change in RH allows rapid adsorption, before crystallisation, and desorption. The low adsorption after exposing the sample to 100% RH confirms that the amorphous lactose has been transformed to crystalline lactose.

2.7.9 Isotherm Method

Bronlund (1997) showed that the isotherms of a mixed sample of amorphous and crystalline lactose can be determined from addition of their individual isotherms. By measuring the free moisture and water activity one can compare with the calculated isotherms to determine the amorphicity of a sample (Billings, 2002; Bronlund, 1997). Alternatively, one can measure the isotherm of the sample and fit the BET model and use the monolayer moisture parameter to determine amorphicity (Vollenbroek et al., 2010). This technique works best for low levels of amorphous lactose.

2.7.10 Relative Humidity

A method for measuring sorption using a fluidised bed of granular materials provided results for silica gel (Gabbott et al., 2003). The sample is first dried, and then a known amount of water added and the relative humidity measured. It may be possible to do this method in reverse, measuring the amount of dry air added to wet amorphous lactose then measuring the RH. In recent experiments, measuring the change in vapour pressure was found to be difficult, and ultimately unsuitable to quantify low levels of amorphicity in spray-dried lactose (Newell et al., 2001). A suggested cause was water being trapped in the crystalline mass.

2.7.11 Glass rod method

One method for measuring the convective drying of single droplets is using a glass filament (Lin & Chen, 2002). A small single droplet was suspended on a glass rod and the temperature and diameter (±1.5% for a 1.6 mg droplet) monitored using a camera. A vertical drying column with controlled hot air flow is used to dry the sample. The moisture content can then be determined. If a flexible long glass filament is used the deflection can also be correlated with

the mass change of the droplet. The calibration of the mass change and deflection was accurate to ± 0.03 mg (balance accuracy 0.02 mg). However, with continuous air flow it is necessary to correct for the drag force of the droplet and glass rod. The resultant mass accuracy was 0.04 mg.

2.8 Amorphous lactose crystallisation

2.8.1 Products of amorphous lactose crystallisation

Bronlund (1997) stated that at low water activity (< 0.55) β-lactose or α-lactose anhydride will form. At higher water activities (> 0.55) there is sufficient water available for lattice water and for α-lactose monohydrate to form. Provided sufficient water is available, α-lactose monohydrate forms preferentially at lower temperatures while β-lactose forms preferentially at higher temperatures (Bronlund, 1997; Nijdam, Ibach, Eichhorn, & Kind, 2007). Schmitt et al. (1999) findings show that at a relative humidity of 57.5% amorphous lactose crystallisation resulted in a mix of α-lactose monohydrate and β-lactose anhydride. Miao & Roos (2005) also found that α-lactose monohydrate, anhydrous β-lactose and anhydrous α-lactose in molar ratio 5:3 and 4:1, stored at 54.5%, 65.6%, 76.1% RH, crystallised from freeze-dried amorphous lactose.

Nijdam et al. (2007) used X-ray diffraction to study amorphous lactose crystallised over a range of temperatures and humidities. They suggest that the advantages of quicker crystallisation times at higher temperatures are offset by the production of less stable lactose forms under storage conditions. For pure amorphous lactose at temperatures ranging from 50 to 110°C at 50% RH the composition was relatively unchanged with 20% anhydrous β-lactose and negligible amounts of α-lactose monohydrate. Composition was also relatively insensitive to relative humidity with a constant 22% for anhydrous β-lactose over the temperature range with α-lactose appearing at only low temperature (50°C). The remainder was mostly anhydrous α-lactose and mixed anhydrous forms of α and β lactose in molar ratios of 5:3, 3:2 and 4:1. Anhydrous lactose crystals with a molar ratio of 5:3 are unstable at low temperatures and high humidities and they recrystallise to the more stable hydrate form, α-lactose monohydrate. For pure lactose the rapid crystallisation time (2-20 min) prevented mutarotation between isomeric forms and α-lactose had very little time for hydration to α-lactose monohydrate. The presence of proteins and salts in whey powders reduced crystallisation rate so that mutarotation and crystal hydration could occur.

2.8.2 Diffusion

2.8.2.1 Introduction

Water adsorption is important due to its plasticising effect that allows the lactose molecules to flow, and eventually crystallise. Figure 2-7 shows the rapid adsorption of dried amorphous lactose, before a stabilising period and desorption. The sorption behaviour for amorphous lactose was shown to be different at 40% RH and 50% RH (Buckton & Darcy, 1996). At 40% RH the sorption behaviour was biphasic with a slow region of adsorption bounded by exponential regions. Buckton also showed that the rate of desorption after crystallisation was a function of the surface concentration (i.e. higher at 0% RH than 20% RH).

During crystallisation, via exposure to high humidity, there is typically a concentration gradient through the amorphous lactose sample due to water adsorption at the surface (Bronlund, 1997; Buckton & Darcy, 1995). In an amorphous powder bed, absorption of water is faster than the rate of supply of water vapour thus the surface does not saturate immediately. Eventually, the centre layers have sufficient moisture content to reduce the driving force for moisture transport so that the rate of adsorption may exceed that of moisture transport. Thus, the surface becomes saturated and starts to crystallise. Expulsion of water from the surface gives rapid vapour supply, which in turn saturates inner layers that also crystallise (Buckton & Darcy, 1995).

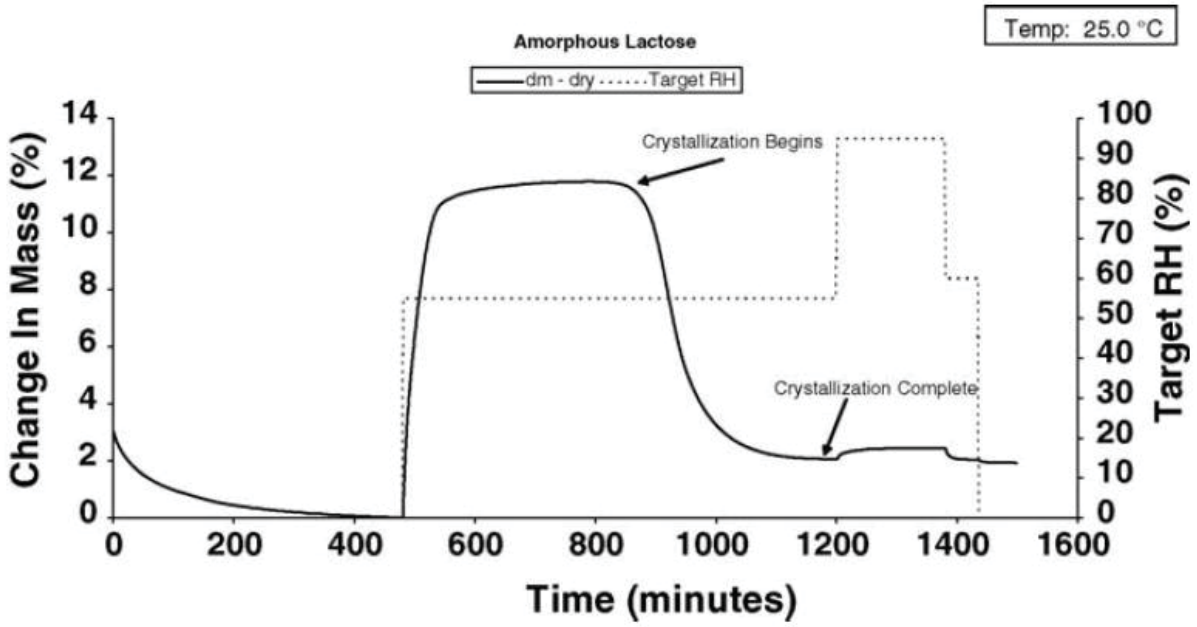

Figure 2-7: Amorphous lactose crystallisation at 55% RH and 25°C (Burnett et al., 2006).

2.8.2.2 Discussion

Bronlund (1997) presents a model for sorption into a thin layer of amorphous lactose around a crystalline particle. Estimates from 0.3 to 0.6 µm for the thickness of the amorphous layer were determined. The model used Fick's law of diffusion to describe moisture transfer through the amorphous layer. A graph of fraction unaccomplished change against time shows that thinner layers had lower sorption times (for 90% sorption: 0.29 µm, 3 s; 0.56 µm, 12 s). However, as noted by Bronlund (1997) and Buckton & Darcy (1995), if crystallisation is occurring this could change the sorption rate. Moisture could be released and the outer surface of the amorphous layer would be at higher moisture content than further into the layer.

A model of moisture sorption onto a bed of lactose was constructed by Ripberger (2011). The results suggested absorption onto the lactose particles was not limiting as there was no significant difference between fitted diffusion coefficients for the 10% and 30% lactose solution. A model of moisture sorption under predicted experimental data for sorption time suggesting diffusion is not limiting. It assumed instantaneous adsorption focusing on diffusion rates, and could have also misjudged the effect on moisture absorption and the change in a_w of the lactose particle. The decrease in relative humidity due to moisture absorption may have an effect on moisture sorption, reducing the driving force.

Ripberger (2010) modelled the time taken for a sphere of amorphous lactose (710 µm) to have moisture diffuse to the centre (99.9% moisture change) and for heat transfer to the centre (99.9% temperature change). Values of 2.5 hours and 142 seconds respectively, were obtained. The time to reach 0.1% crystallinity using the Avrami equation was also accounted for, $T–T_g$ = 35°C, t = 114 seconds.

2.8.3 Crystallisation kinetics

2.8.3.1 Introduction

There is a tendency for many substances to crystallise because the overall energy is reduced. Crystalline structures can be formed through crystallisation of amorphous substances which are meta-stable systems (Palzer, 2010). Figure 2-8 outlines the two stages of crystallisation of amorphous materials in spray dryers. First, there is the possibility of crystallisation in the liquid phase as the droplet dries out and solids concentration increases. Secondly, there is the process known as solid phase crystallisation, where any amorphous material is transformed to a crystalline form. It is this stage which is likely to be governed by the Avrami or WLF equation outlined below.

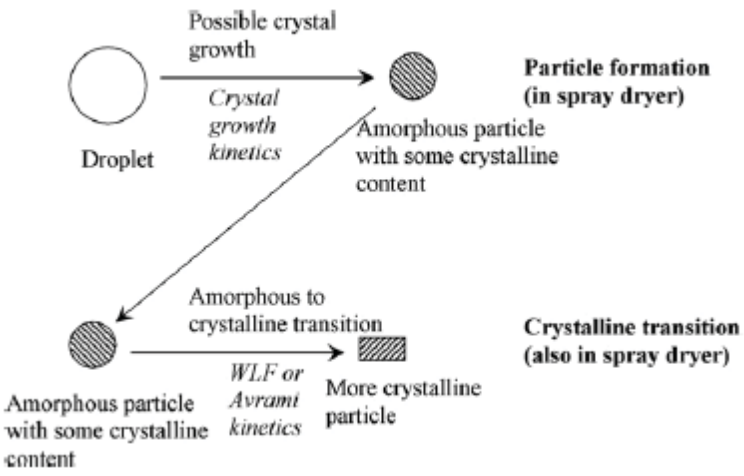

Figure 2-8: Crystallisation stages in spray dryer (Langrish, 2008).

2.8.3.2 Avrami equation

The Avrami equation is often used to describe the kinetics of crystallisation (Saunders et al., 2004). Equation (5) shows a simplified form of this. It assumes the nucleation rate is independent of amount crystallised and that crystal growth is linear with time.

$$1 - Y = Y_{cr} = 1 - \exp(-K\, t^n) \tag{5}$$

The crystallised fraction is (1 − Y), equal to Y_{cr}, concentration of crystallised substance based on the total mass of substance able to crystallise. K is a constant containing the nucleation and growth rate; while n is the Avrami exponent with a theoretical value of 2. Equation (5) shows a sigmoidal dependency between time and crystallised mass. These kinetics correspond to a limiting nucleation at the start and a decreasing crystallising concentration near the end of crystallisation (Palzer, 2010).

The crystallisation kinetics are dependent on the molecular mobility of the system, and the molecular mobility dependent on temperature. As mentioned, water acts as a plasticiser increasing molecular mobility and reducing T_g. However, dilution of a system can also reduce nucleation rate due the lower number of contacts between crystallising molecules (Palzer, 2010).

2.8.3.3 WLF Equation

The Williams-Landel-Ferry (WLF) equation relates relaxation time of mechanical properties to the temperature above the glass transition temperature (T_g) (Williams, Landel, & Ferry, 1955). Changes in viscosity in a polymer due to the glass transition can be related to the temperature above the glass transition temperature.

$$\frac{\mu}{\mu_g} = \frac{-C_1(T - T_g)}{C_2(T - T_g)} \tag{6}$$

The WLF equation can be applied to conditions that give both drying and crystallisation. It takes into account that the rate of crystallisation is related to the temperature difference ($T–T_g$) between the material and the glass transition temperature. A DSC was used to show the rate of crystallisation of amorphous lactose agreed well with WLF kinetics (Roos & Karel, 1990, 1992). Crystallisation time, t_{cr} was the time at which heat flow reached a maximum and t_g was the average crystallisation time at T_g.

$$\log_{10}\left(\frac{t_{cr}}{t_g}\right) = \frac{-17.44\ (T - T_g)}{51.6 + \ (T - T_g)} \tag{7}$$

2.8.3.4 Avrami-Bronlund Equation

Bronlund (1997) presented a model for amorphous lactose crystallisation based on the differentiated form of the Avrami equation shown below.

$$\frac{d(1 - Y)}{dt} = n_A K_A Y \left[\frac{-\ln Y}{K_A}\right]^{\frac{n_A - 1}{n_A}} \tag{8}$$

When nucleation is not rate limiting, as in amorphous lactose, the rate constant is given by the equation below.

$$K = C_3\ (\exp\left(\frac{-C_1}{R\ (C_2 + T - Tg)}\right))^3 \tag{9}$$

Bronlund (1997) found n_A to be 3, interpreted to mean that growth was linear in 3 dimensions. Equation (8) includes the WLF equation that accounts for the change in viscosity with $T–T_g$.

2.8.3.5 Discussion

Kedward et al. (2000) used a DSC and the Avrami equation to show that the highest maximum crystallisation rate for freeze dried amorphous lactose were from the samples with the highest moisture content (lowest T_g).

Burnett et al. (2006) investigated the rate of spray dried amorphous lactose crystallisation using gravimetric vapour sorption experiments. The onset of crystallisation was assumed to occur when the slope of the mass versus time graph turned negative (i.e. sorption peak). Modelling software and multiple curve fitting found two competing 2-step processes for crystallisation above 25°C at 51% RH. Burnett suggested that in each case the auto-catalysed first step was nucleation and the second was water diffusing out of the lactose. Physically, water is liberated as crystallisation occurs and the resultant reduction in viscosity in the amorphous matrix accelerates crystallisation (Palzer, 2010).

Miao and Roos (2005) used the Avrami equation to model the crystallisation of spray dried lactose. Using XRD, the Avrami equation fitted well to data and $t_{1/2}$, the time for 50% crystallisation, ranged from 25 hours to 4-6 hours for 54.5% and 76.1% RH respectively, at 22°C.

Ibach and Kind (2007) studied crystallisation kinetics of amorphous lactose at high temperatures. Temperatures ranged from 50°C to 110°C and humidities from 20% to 80% RH. The setup was a balance within a controlled humidity chamber with an external heating jacket. They showed that higher temperatures and humidities resulted in faster crystallisation times. Crystallisation times ranged from 1 min to 100 min. They used gravimetric analysis and assumed crystallisation began at the onset of the moisture decrease after the sorption peak. Given that sorption time was a significant proportion of total crystallisation time, it is likely the surface layers of amorphous lactose were first to saturate and crystallise. Thus, crystallisation would be occurring before the sorption peak as was assumed. Using IR to follow DVS experiments has found that water desorption may precede crystallisation and crystallisation may complete before sorption levels off (Gustafsson et al., 1998).

Langrish (2008) presented a comparison between the data given by Ibach & Kind (2007) and the WLF equation. If WLF kinetics were followed, the rate of crystallisation should have been constant for different relative humidities. Langrish checked two cases, crystallisation starting at initial exposure of the sample or from the sorption peak; it made no difference, the crystallisation rates calculated using the WLF equation were different. A different approach, using $T-T_g$ and the degree of crystallinity, assuming 0% crystallinity at peak sorption and 100%

at the final moisture content, was used. Figure 2-9 graphs the ratio of the rate of change in crystallinity to the rate of change at T_g against $T-T_g$. The experimental data and the WLF equation both show a large increase in reaction rate at a $T-T_g$ between 30 and 35°C. However, when the data from Ibach & Kind was plotted in this fashion it did not agree with the WLF equation. Reasons suggested were that the rate of moisture loss is not exactly the same as the crystallisation rate or because $T-T_g$ did not exceed 30°C.

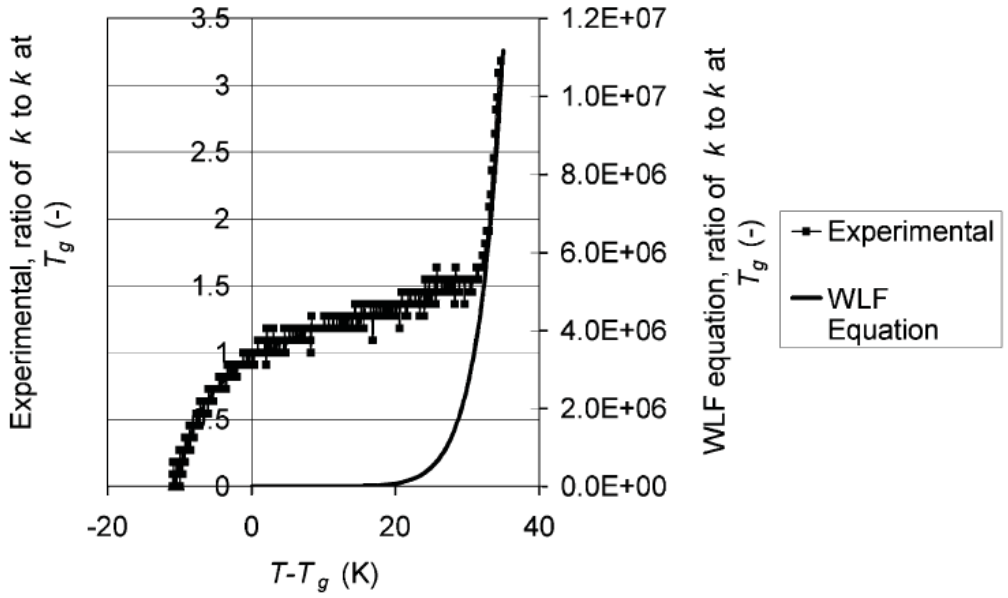

Figure 2-9: Experimental ratio of the rate of change in crystallinity (k) to the rate of change at T_g (k at T_g) for spray dried lactose, along with the ratio from the WLF equation as functions of $T-T_g$ (Langrish, 2008).

Langrish and Wang (2009) show the difference between the rates of crystallisation for sucrose and lactose at 75% RH and 40°C is minimal. Because lactose and sucrose have different T_g, the results contradict the WLF equation. However, due to the high operating humidity the similarity may be because the water sorption was the limiting factor and not the rate of crystallisation.

During drying the T_g of the lactose droplets will increase as water is removed. Lower drying temperatures can result in higher residual moistures, giving a higher $T-T_g$ during the latter drying stages (Fu, Woo, Moo, & Chen, 2012). However, during the critical stage of drying, when crystallisation occurs, the $T-T_g$ will be much higher and higher temperatures will promote a higher $T-T_g$. The increase in crystallisation rate as $T-T_g$ increases predicted by WLF kinetics should be followed. Increasing the inlet air temperature of a spray drier was found to increase crystallinity from ~55% to ~76% (Chiou & Langrish, 2008). Another spray drying setup also found that that the rate of lactose crystallisation increased as $T-T_g$ increased using a spray

drying system for inlet gas temperatures from 200°C to 170°C (Whiteside et al., 2008). A single droplet drying technique (see 2.7.11) found higher crystallinity for a drying temperature of 110°C compared with 70°C for single droplets despite shorter drying time for the higher temperature (Fu et al., 2012).

Das and Langrish (2012) showed that the WLF equation is inconsistent and cannot account for the effect of moisture change on crystallisation rate. The WLF equation assumes a constant $T-T_g$, but as moisture content changes T_g varies. They present an activated rate equation based on the Eyring equation that correlates enthalpy and entropy of activation with crystallisation rate.

Bronlund (1997) found values for the constants in equation (9) by fitting the model to experimental data and that of Roos and Karel (1990, 1992). Brooks then refitted the model including further data from Schmitt et al. 1999. Figure 2-10 shows the WLF model and the Avrami model well as data from several experiments (Bronlund, 1997; Brooks, 2000). The graph shows that only with a $(T-T_g)$ of about 40°C does crystallisation time reduce below an hour. The modified Avrami model predicts crystallisation time better than the WLF equation for low $(T-T_g)$ driving forces.

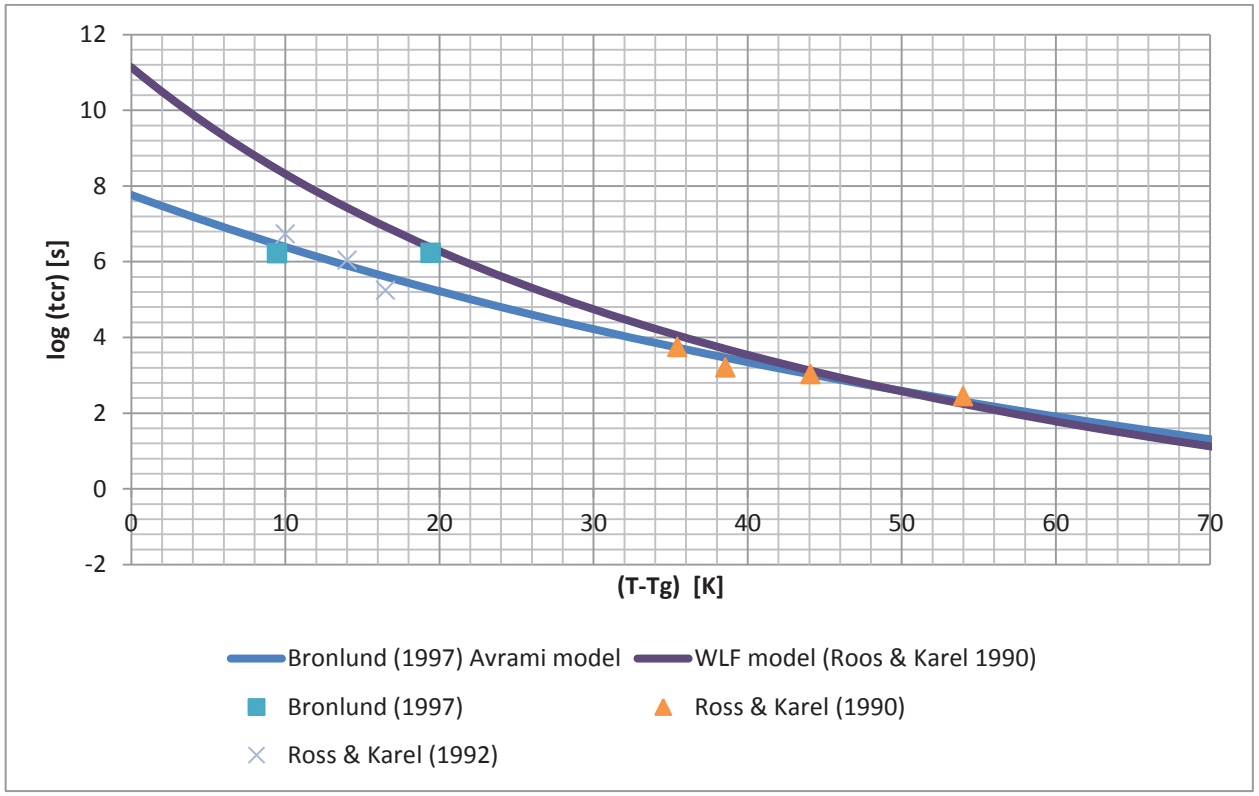

Figure 2-10: Time for 90% crystallisation versus $T-T_g$.

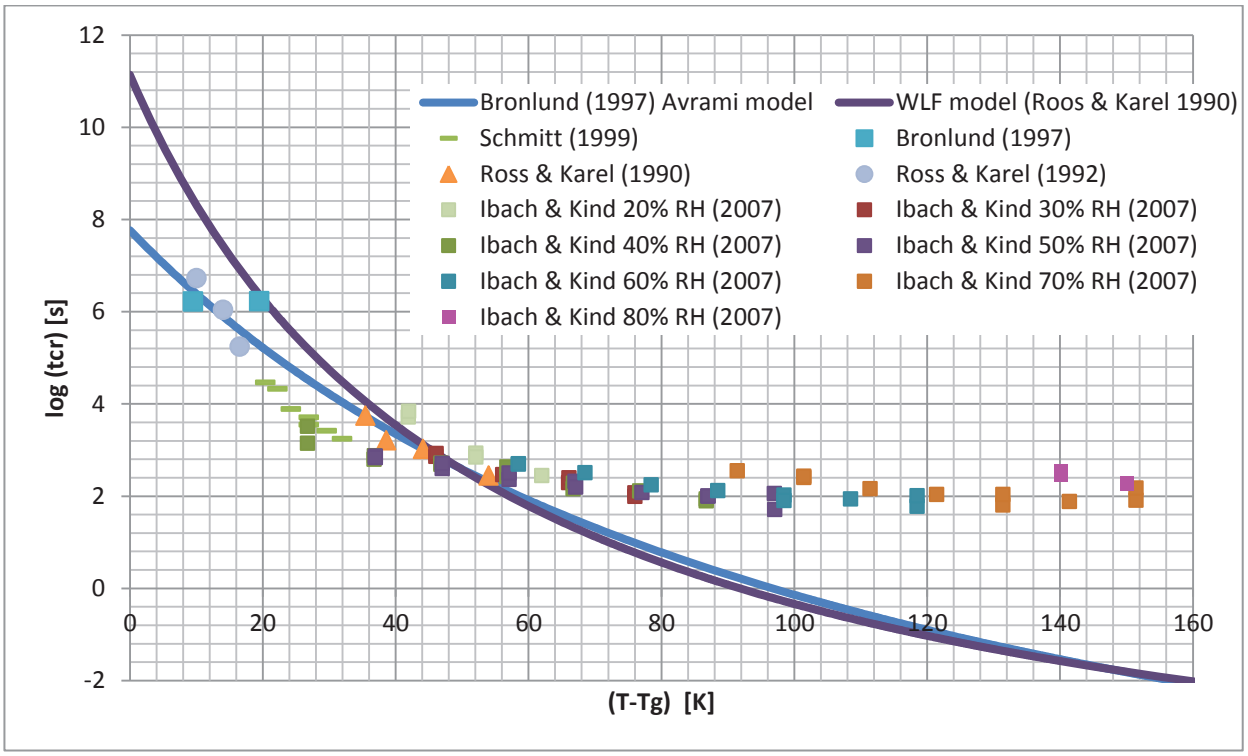

Figure 2-11:Time for 90% crystallisation versus $T-T_g$ including Ibach & Kind data.

In Figure 2-11 the data from the recent study of Ibach and Kind (2007) is included along with the Avrami and WLF models. With the exception of that recorded at 20% RH, the data does not follow the model. Crystallisation time is relatively constant and underestimated by both models at $T-T_g$ values greater than 60 degrees ($t \sim 12$ s). The results suggest there is a minimum crystallisation time and that the models are not valid at $T-T_g$ values greater than 60°C.

2.9 Fluidisation

To prevent caking of lactose based powders it has been recommended that the amorphous fraction be crystallised after spray drying (Ibach & Kind, 2007). A fluid bed dryer has high heat and mass transfer rates and low residence times. Either the inlet temperature of the fluidised dryer, or the air humidity, must be raised in order for the temperature to be greater than T_g and there to be a driving force for crystallisation. A common problem is that operating at the high humidity required causes the collapse of the bed due to sticking (Palzer, 2005).

Nijdam et al (2008) investigated the limits of fluidisation of several whey powders with various degrees of crystallinity. The experimental setup used a vibrated fluidised bed with a bubble column and heater in series to generate hot humid air. They first found the humidity limit above which the powder became too sticky to fluidise. Any increase above the fluidisation limit resulted in immediate agglomeration and then channels in the bed with mixtures of partially

and fully crystallised whey powder. Partially amorphous whey powder was shown to be only able to be fluidised up to a relative humidity of half that of fully crystallised powder at any given air temperature. They suggest it is possible to fluidise 25°C to 40°C above T_g for partially crystalline whey powder depending on the air relative humidity, but would take, according to Ibach and Kind (2007), at least 100 minutes to crystallise. This is considerably longer than industrial processes used for drying of lactose. However, they showed that coating the sticky partially crystallised lactose with non-sticky crystalline lactose allowed fluidisation to occur at higher humidities. Yazdanpanah & Langrish (2011) found at the lab scale a 83% and 100% improvement in crystallinity at 60°C and 40% RH after 30 and 60 minutes respectively, using a vibrated fluidised bed. The limits to fluidisation for amorphous lactose ranged from about 78°C at 36% RH and 60°C at 48% RH. Using equation (3) this gives $T-T_g$ values of 50.7°C and 44.8°C. Figure 2-12 shows the fluidisation limit for both studies. It is surprising that the amorphous lactose has a higher fluidisation limit than the partially crystallised whey powder. The fluidisation limit for amorphous lactose varies widely between studies. This may be due to variation in bed design or conditions allowing collapse at different T_g. Also, collapse points are often measured visually introducing variation.

Another approach is to examine the point when stickiness develops between particles, which precede caking and collapse. A study using lactose/protein mixtures showed a $T-T_g$ of 10°C and 90°C before sticking occurred for 15.5% and 83.4% protein respectively (Hogan & O'Callaghan, 2010). Work to independently measure the stickiness of amorphous lactose with a special rig, rather than fluidised bed, found that above a $T-T_g$ of 25°C, stickiness developed almost instantaneously (Paterson et al., 2005).

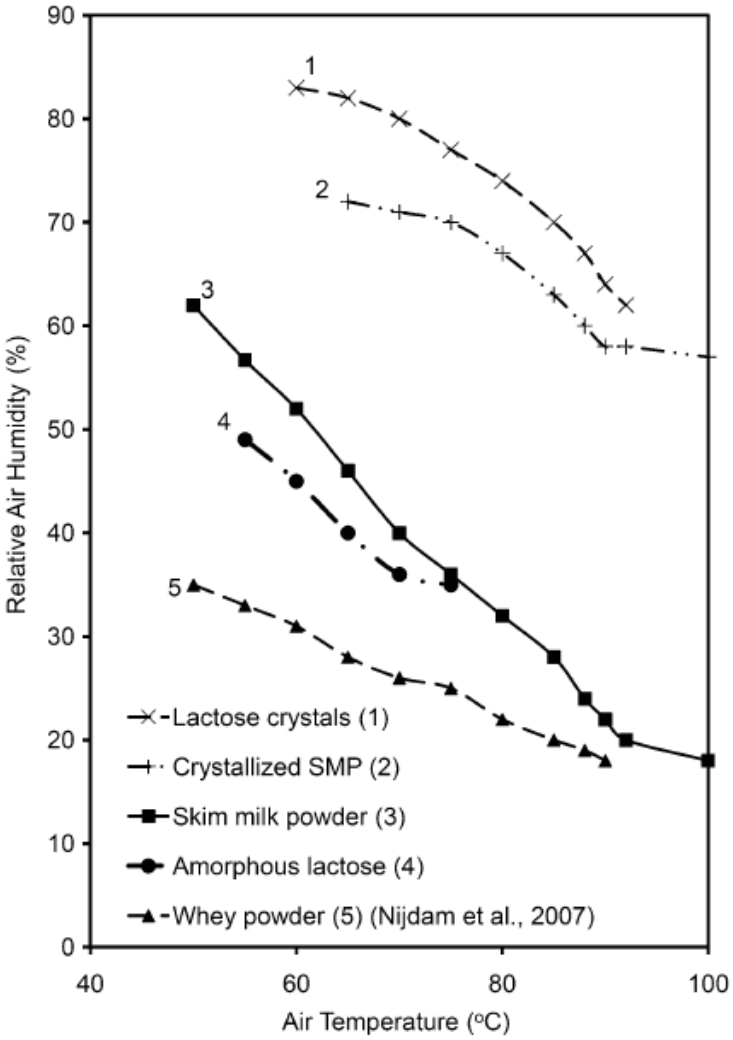

Figure 2-12: Upper limits for fluidisation for process air under lactose (Yazdanpanah & Langrish, 2011).

2.10 Possible Methods

To track the crystallisation reaction, temperature and humidity must be controlled. Isothermal techniques such as the TAM, allow only humidity to be varied. The TAM also has the limitation that it measures amorphous lactose though the energy of a complete crystallisation, preventing the study of amorphous lactose crystallisation as a time dependent process.

The glass rod method, described in section 2.7.11, is a viable method for observing single droplet drying and perhaps crystallisation kinetics. It has been developed over several years and the associated experimental setup for the glass filament is relatively difficult. Dehumidified air is used and the pressure finely tuned with an associated heating chamber. For recording the results through the wall of the heating column a video camera, with enough lenses for appropriate magnification and suitable post processing software, is required. Also required is a delicate glass filament with suitable tip size. Thermocouples are attached to the

glass tip. The volume of solution used was only 1-5 µL. There may also be difficulties in measuring the amorphous content of such a small sample. The technique has been used to monitor the moisture content of glucose (calculated from diameter and physical properties) over time (Che & Chen, 2010). The method is likely to be unviable in the timeframe allowable.

One approach would be to construct a reaction vessel, similar to a fluidised bed with temperature and humidity sensors. Starting with wet amorphous lactose the drying and crystallisation rate could be measured simultaneously. By measuring amorphicity before and after drying the crystallisation rate could be isolated. As mentioned earlier, inducing crystallisation at high humidities in fluidised beds often causes caking and collapse of the bed. Also, the fluidisation limit maybe as low as a $T-T_g$ of 25°C. Using lactose samples with only a thin amorphous layer, rather than pure amorphous lactose, is unlikely to have an effect on the fluidisation limit. As mentioned in section 2.9, one estimate of the crystallisation time at the fluidisation limit was 100 minutes, which is roughly an order of magnitude higher than industrial crystallisation times. Therefore, the experimental conditions that simulate those of the reference plants probably cannot be achieved with this method.

A reaction vessel could be developed where the sample is subjected to tightly controlled temperature and RH conditions and then removed for analysis. The samples would need to be suspended during the period when they are removed from the reaction vessel and placed into an analyser. To enable measurement of the degree to which crystallisation has occurred, crystallisation must be halted; this could be done by rapidly cooling the sample.

The above approach could use a small sealed container in which a monolayer of lactose particles are placed. The container should be made out of a conductive material with high melting point e.g. stainless steel. The particles would be equilibrated at the appropriate relative humidity to achieve the desired water activity. The container would then be placed in a high temperature environment e.g. water bath or oven and allowed to crystallise. The container is then removed after a recorded amount of time and suspended by rapid cooling e.g. by placing in excessive liquid nitrogen. The sample can be later analysed for amorphicity.

The above method is similar to the conventional DSC method. DSC pans containing lactose samples have been subjected to an abrupt temperature change by isothermal heating. In DSC, the heat flow is measured, allowing the amorphicity at any time value to be determined (Bronlund, 1997). The problem with this method is achieving the appropriate humidity

conditions in the pan. This can be done using salt solutions, but is then limited to the humidity conditions supplied by the salts.

The advantage of using salt solutions over having a sealed container is that some of the desorbed moisture will be absorbed by the salt rather than remaining and affecting the reaction kinetics.

By not measuring amorphicity in situ the experimental setup is simpler and allows more flexibility in equipment use. After comparing the sealed reaction vessel with the other methods, it is judged as the most viable considering the timeframe and equipment available.

2.11 Conclusion

The kinetics of amorphous lactose are important in determining the fluidised bed operating conditions required in order to have complete transformation to crystalline lactose. The point above which amorphous lactose can crystallise is the glass transition temperature (T_g), where the viscosity of lactose reduces, and molecular mobility increases. Water acts as a plasticisation agent, lowering T_g. The literature shows there is a positive relationship between the temperature above T_g, $T-T_g$, and the crystallisation rate. The WLF and Avrami-Bronlund model both includes terms for $T-T_g$, showing it is the most important property in crystallisation kinetics. In this work crystallisation kinetics will be measured and the results compared with the WLF and Avrami-Bronlund models. A sealed reaction vessel with subsequent amorphicity analysis was selected as the most viable method.

3 Method Development

3.1 Experimental Range

The work in this project aims to use the conditions of two industrial lactose plants as a reference for determining the kinetic of amorphous lactose crystallisation during the drying of alpha lactose monohydrate. The conditions in two commercial lactose plants, with a focus on the drying stage, are shown below.

Plant A – Vibrated fluid bed, Inlet air: 110°C Outlet: 90-95°C

Plant B – Vibrated fluid bed, Inlet air: 150°C Outlet: 85-90°C

Because the temperature difference in the fluidised bed at Plant B is higher than that of Plant A it is likely that there is more drying occurring. The plant data are further investigated in the mass balance that follows.

3.1.1 Mass and Energy Balance of Industrial Process

In the production process of lactose, concentrated whey passes from an evaporator to a crystalliser (Figure 2-2). After the washing step, which involves centrifugation, the lactose is dried. The drying process involves crystalline lactose dropping from a centrifuge through a flash dryer then a fluidised bed. A mass balance can be constructed, around each drying process, and for the overall drying system.

The first balance is around the flash dryer, the next balance is around the fluidised bed, and the last around the cooling side of the fluidised bed.

The process flow diagram below details each stream.

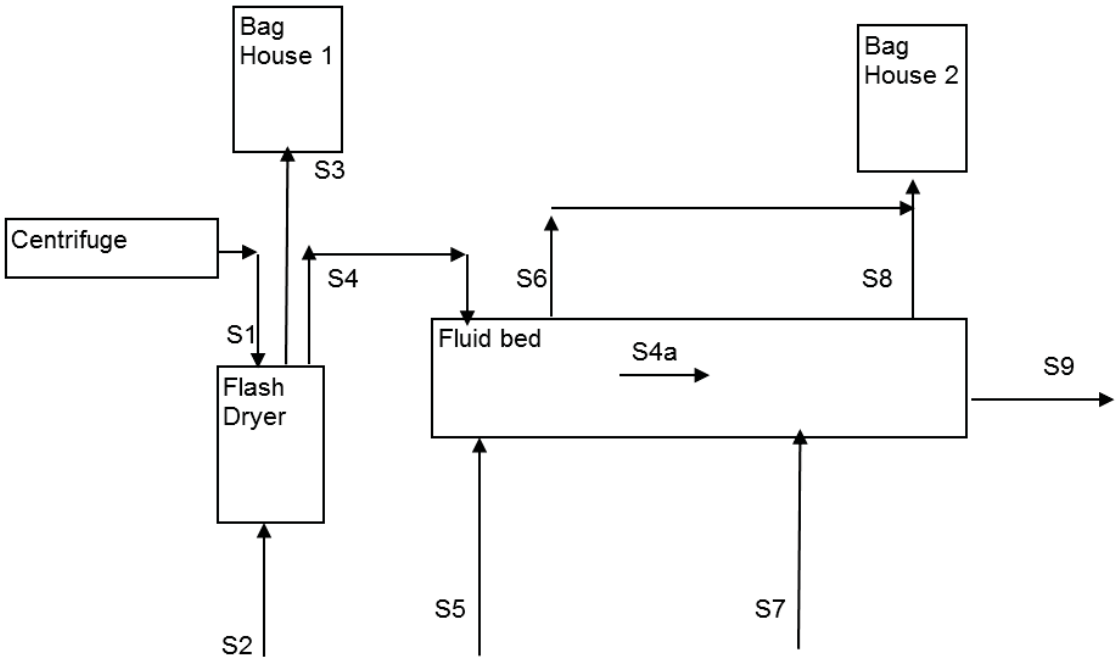

Figure 3-1: Process flow diagram of lactose plant drying system.

The following assumptions apply to both mass balances:

- Standard enthalpy and heat capacity data with a datum of 0°C.
- The exit temperature of the product leaving the fluidised bed is the same as the air stream.
- Water coming in with the air stream is ignored.
- Cooling air flow rate specified is assumed to equal heating air flow rate.

Assumptions specific to each plant are shown in Table 5 and Table 6.

Shaded cells indicate the variables changed to solve the balances.

Table 3: Mass balance for Plant A

Stream	S1	S2	S3	S4	S4a	S5	S6	S7	S8	S9	S4b	S4ba	S5b	S6b	S7b	S8b	S9b
	Flash dryer				Fluidised bed (large)						Fluidised bed (small)						
Lactose (kg/s)	1.67	0	0	1.11	1.11	0.00	0.00	0.00	0.00	1.11	0.56	0.56	0.00	0.00			0.56
Air (m3/s)		9.00	9.00	0.0	0.0	4.25	4.25	4.25	4.25	0	0	0	4.60	4.60	4.60	4.60	0
Water (kg/s)	0.10	0	0.10	0	0	0	0.0	0	0	0	0.0	0	0	0.0			0
Total (kg/s)	1.76	9.00	9.10	1.11	1.11	4.25	4.25	4.25	4.25	1.11	0.56	0.56	4.60	4.60	4.60	4.60	0.56
Total (m3/s)		9.00				4.25		4.25					4.60		4.60		
Temperature (°C)	30	147.9	105	95	97.9	110	97.9	27.5	42.7	32.7	97.9	151.4	165	151.4	27.5	43.6	43.6
Range temp. (°C)		140-165	100-110				90-95	25-30	30-60				160-170		25-30		30-40
Density (kg/m3)		1.18	0.91			1.18			1.10				1.18			1.09	
Heat (kW)																	
Heat in lactose	62.5	0	0	131.9	135.9	0	0	0	0	45.4	68.0	105.2	0	0	0	0	30.3
Heat in Air	0	1344.6	954.5	0	0	472.2	420.1	118.0	183.3	0	0	0	766.6	703.5	127.8	202.8	0
Heat in water	12.2	0	258.7	0.44	0.23	0	1.45	0	0	0.08	0.23	0.18	0	0	0	0	0.01
Total heat	74.7	1344.6	1213.1	132.4	136.2	472.2	421.6	118.0	183.3	45.5	68.2	105.3	766.6	703.5	127.8	202.8	30.3
Heat losses			141.9				72.3			25.4					25.9		23.3
Balances			0.0				0.0			0.0					0.0		0.0

Table 4: Mass balance for Plant B

Stream	S1	S2	S3	S4	S4a	S5	S6	S7	S8	S9
	Static fluidised bed				Vibrated fluidised bed					
Lactose (kg/s)	1.39	0	0	1.39	1.39	0	0	0	0	1.39
Air (m^3/s)		4.72	4.72	0	0	8.85	8.85	8.85	8.85	0
Water (kg/s)	0.15	0	0.11	0.04	0.001	0	0.04	0	0	0.001
Total (kg/s)	1.54	4.72	4.83	1.43	1.39	8.85	8.89	8.85	8.85	1.39
Total (m^3/s)		4				7.5		7.5		
Temperature (°C)	15	146.3	50	50	106.6	150	106.6	20	29.0	29.0
Range temp. (°C)		150				150	85-90	15-30	30-60	
Density (kg/m^3)		1.18	1.07			1.18			1.14	
Heat (kW)										
Heat in lactose	26.0	0	0	86.8	185.1	0	0	0	0	50.3
Heat in Air	0	697.4	238.4	0	0	1340.8	953.2	178.8	259.2	0
Heat in water	9.68	0	289.0	8.98	0.31	0	110.2	0	0	0.08
Total heat	35.7	697.4	527.3	95.8	185.4	1340.8	1063.4	178.8	259.2	50.4
Heat losses				110.0			242.3			54.6
Balances				0.0			0.0			0.0

Table 5: Mass balance assumptions for Plant A

Description	Value	Unit
Basis of feed	6	T/hr
Free moisture content out on centrifuge	10.0%	total wt basis
Free moisture content out to fluid bed	0.1%	total wt basis
Free moisture content out of fluid bed	0.05%	total wt basis
Concentration of alpha-lactose monohydrate in solution on crystals	19.433	g L/100 g water
Amorphous % expected on surface	1.12%	
Air heat losses	10%	
Large fluid bed	4	T/hr
Small fluid bed	2	T/hr

Table 6: Mass balance assumptions for Plant B

Assumptions	Value	Units
Basis of feed	5	T/hr
Free moisture content out on centrifuge	10.0%	total wt basis
Free moisture content out to fluid bed	3%	total wt basis
Free moisture content out of fluid bed	0.05%	total wt basis
Concentration of alpha-lactose monohydrate in solution on crystals	16.8	g L/100 gwater
Amorphous % expected on surface	1.83%	
Air heat losses	15%	

The hot air inlet temperature for the fluidised bed is 110°C and 150°C for Plant A and Plant B respectively. The inlet air stream for the flash dryer (stream 2), outlet air stream (stream 6) and the cooling air outlet temperature (stream 8) were the variables solved to make the balances to equal zero. Although the inlet air temperatures for the two plants were similar at 146.3°C and 147.9°C, the outlet temperatures were very different at 50°C and 105°C respectively. The drying process is different between the plants. The heat going out in the air of the baghouse stream for Plant B is 238.4 kW compared with 954.5 kW for the Plant A, even though the heat in the water is roughly the same. More drying is occurring during the flash drying at Plant A than at Plant B.

The fluidised bed outlet air temperature was found to be 97.9°C and 106.6°C for the Plant A and Plant B large fluidised beds respectively. There is much more drying occurring in the Plant B fluidised bed with 110.2 kW of heat energy in the lactose compared with close to zero in the Plant A streams.

The balances show there is more drying during the flash dryer at Plant A than Plant B. Subsequently, there is more drying in the fluidised bed at Plant B than Plant A.

From the literature review, we know $T-T_g$ is an important kinetic property, present in both the WLF and Avrami kinetic models. The range of conditions can be estimated as a function of $T-T_g$ by substituting the moisture content into the dryer and the outlet air temperature into equation (4).

Plant A: T = 97.9°C, T_g = 66.3°C (MC = 2%), $T-T_g$ = 31.6°C.

Plant B: T = 106.6°C, T_g = 50.5°C (MC = 3%), $T-T_g$ = 56.1°C.

This can only be considered a rough approximation as the moisture content of the particles entering the drying system is highly variable. Because the lactose comes out of the Plant A fluidised bed with less moisture the T_g of the particles are higher. This leads to a lower $T-T_g$; therefore, there is a greater potential for amorphous lactose to remain after the drying process.

3.2 Preparing Amorphous Lactose

A completely amorphous lactose powder was used as it is easier to reproduce than a crystalline/amorphous blend. Two methods exist for this production of this powder, freeze drying or spray drying. This work aims to vary the humidity to allow crystallisation to occur, the diffusivity of water through freeze dried lactose is higher than that through spray dried lactose and thus will take a shorter time to reach equilibrium. An estimate of the time taken for 200 μm particles freeze dried to achieve 99.9% moisture change to the centre, using Ripberger (2010) diffusivity values, gave 690 seconds compared with 10 days for spray dried lactose. Due to this large variation both powders were used in this work to allow a comparison to be made.

3.2.1 Freeze drying

Freeze drying is a common food dehydration method that consists of three stages: freezing, primary drying and secondary drying. During freezing, the free water in the sample becomes ice. The primary drying step, which is typically the longest, involves the sample being placed

into the chamber of the freeze dryer. A vacuum allows for sublimation of the ice, facilitating removal of unbound water. During secondary drying the sample is slowly heated allowing water that did not freeze to be removed by desorption (Tang & Pikal, 2004). The temperature-time profiles during the three stages can be modified depending on the desired properties of the final product.

Amorphous lactose has been produced from a 10% lactose solution freeze dried for 24 hours at a pressure below 0.1 mbar (Roos & Karel, 1990). 10 g of solution was frozen at -20°C overnight then tempered over dry ice for 3 hours prior to freeze drying. Liquid nitrogen has also been used to rapidly freeze samples which were subsequently freeze dried for 48 hours (Tsourouflis, Flink, & Karel, 1976). The rapid cooling rate of liquid nitrogen makes it a preferred coolant (Tang & Pikal, 2004). Brooks (2000) freeze dried a 10% α-lactose monohydrate solution at -55°C and 250 millitorr over 48 hours.

In this work because of diffusion the particle size distribution of the lactose is important. Two millimetre diameter balls of lactose were created by using a burette to drop lactose solution into liquid nitrogen and subsequent freeze drying at -40°C for 72 hours (Feral, 2010). To improve the control of the particle size, to the micrometer scale, a droplet generator can be used. Lactose solutions of concentration 10%, 20% and 30% were passed through a droplet generator, collected in a liquid nitrogen solution and then freeze dried at -40°C, 0.1 millibar for 4 days (Ripberger, 2010). It was decided to follow this method for the current project because similar equipment was available.

Sieving of the freeze dried lactose particles was carried out in an enclosed box. The box with sieves inside was purged with compressed air (10-12% RH) for 10 minutes prior to sieving. The freeze dried lactose was then passed through a 250 micron sieve in order to remove any large agglomerates.

3.2.2 Spray drying

Spray drying is a common drying method in which a concentrated solution is atomised and contacted with hot air to evaporate the water, producing a powder.

A GEA Niro spray dryer located in the Food Pilot Plant at Massey University was previously used successfully by Ripberger (2010) to produce an amorphous lactose powder. Ripberger feed a 30% w/w solution held in a water bath at 75.3°C, into the dryer with an inlet air temperature of 200°C, the feed rate was controlled to produce an outlet temperature of 91-94°C. To remove any residual moisture and stabilise the powder the samples were then oven

dried at 105°C for 24 hours. In this work these conditions were used as the initial starting point for the preparation of spray dried amorphous powder.

To refine the experimental method a model of the pilot plant spray dryer was used to determine the feed flowrate and thus, outlet temperature (Paterson, 2012). This model uses a mass balance around the spray dryer allowing the $T-T_g$ value to be predicted. The heat balance includes the heat to evaporate water, heating solids and heat losses. Water was run through the spray drier while the inlet and outlet temperatures, and feed and air flowrates were measured. The value for heat losses was adjusted until the model gave the measured outlet temperature. This value was 74% of the total gas heat load, a significant proportion. This is a weakness of the model as a small change in the heat losses value can give a significant change in the $T-T_g$ predicted. Furthermore, as the heat loss value is likely to change non-linearly with increasing outlet temperature this is likely to introduce error. Also, slight changes in the air flow largely affect the $T-T_g$ predicted. The air flow reading with a monometer (10.5 m/s) was fluctuating when taken showing there is uncertainty with this value. Decreasing velocity by 0.5 m/s increased the optimal flowrate from 25 to 30 g/min. The model predicted that there was an optimum flowrate which gave the minimum $T-T_g$ as shown by Figure 3-2.

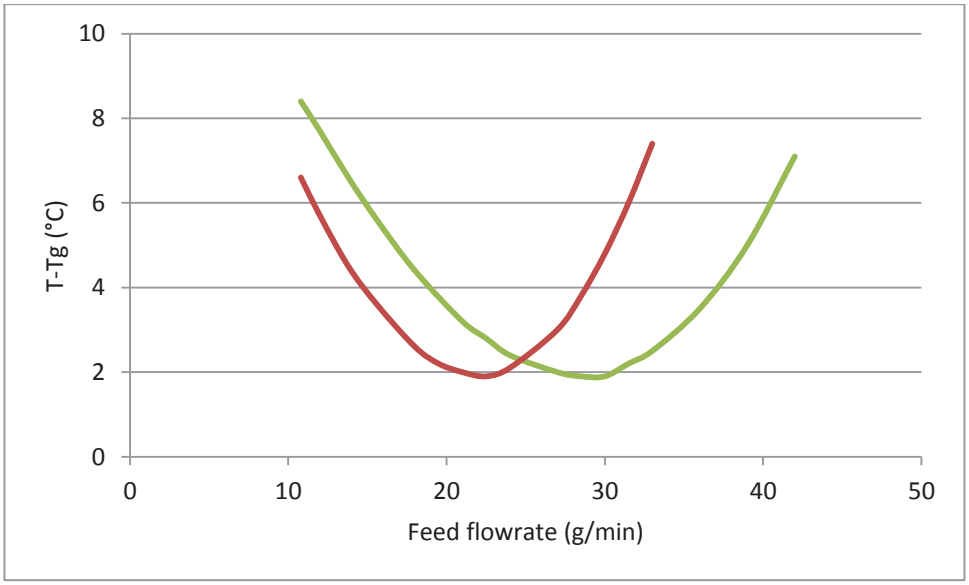

Figure 3-2: Spray dryer flowrate against $T-T_g$.

Figure 3-2 shows the minimum $T-T_g$ occurs at a flowrate of around 30 g/min and 21 g/min for 30% and 10% lactose solution, respectively. Spray dried amorphous lactose was produced at these conditions and stored over desiccant. The amorphous nature of the sample was confirmed using polarised light microscopy and X-ray diffraction (Appendix 8.2).

Experimentally, it was found that much of the lactose was sticking to the walls of the spray dryer, giving only about 50% recovery. This is much lower than in industry and may be due to the smaller size of the dryer. Sticking is an indication that some lactose is at a $T-T_g$ of about 10°C or above. The model predicts a $T-T_g$ of only about 2°C. Some proportion of the lactose stream may have insufficient drying before contacting the walls. Also, caking was present on the walls of the collection jar as well as some condensation forming was found. It was found heating the collection jars helped prevent this.

3.3 Measuring amorphous lactose

The sensitivity of the instruments limits the level of remaining amorphous lactose that can be measured after crystallisation. A HIDEN Isochema DVS and a microcalorimeter, Thermal Activity Monitor (TAM), manufactured by Thermometric (Sweden) were available for use at Fonterra. The DVS uses sorption isotherms to determine the amorphous lactose fraction in a sample. The TAM measures the heat energy released during crystallisation to allow the amorphous lactose to be quantified. Each of these instruments are discussed separately in the sections below.

3.3.1 Thermal Activity Monitor (TAM)

The TAM is a microcalorimeter, based on measuring the heat flow between a reference and a sample. The model used was the 2277 manufactured by Thermometric AB. This can detect heat flows as low as ±50 nW (Bergqvist & Soderqvist, 1999). It is essentially a large, finely temperature controlled water bath (25 ± 0.0001°C). Two ampoule holders allow a sample and a reference to be lowered into the water bath. During an experiment, heat is either produced or absorbed causing a temperature difference measured by the thermopiles. The voltage measured is directly related to the heat flow from the sample.

3.3.2 TAM Method

The method used was the closed ampoule method (Billings, 2002). In this the ampoule acts as a closed system. Inside the ampoule is the sample and a Durham tube of saturated salt solution ($Mg(NO_3)_2$ ~ 53% RH). The power output required to maintain isothermal condition is measured as the sample crystallises. The power range of the TAM was 0-3000 µW.

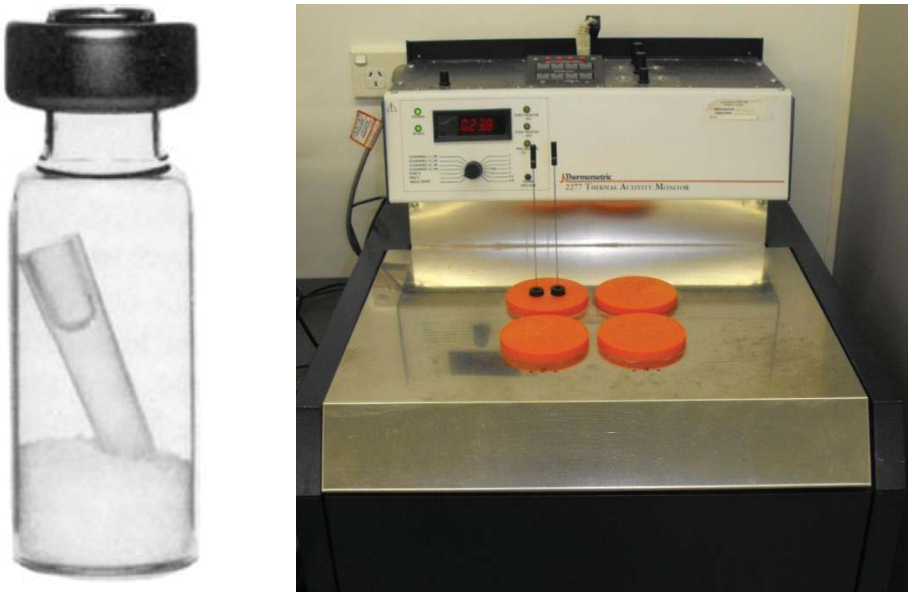

Figure 3-3: Closed ampoule with saturated salt solution (photograph: Thermometric), Thermal Activity Monitor (TAM).

The samples were prepared immediately prior to analysis to prevent crystallisation. All equipment was stored in a humidity chamber below 30% RH and gloves were worn to handle the equipment to prevent any surface moisture contamination. A small amount of lactose (10-100 mg) to be analysed for amorphicity was added to a glass ampoule. A Durham tube half filled with saturated salt solution (54%) was then added. The ampoule was then sealed, crimped and a small hook added to allow attachment to the TAM sample holder.

The DigiTAM software (v4.1), supplied by the manufacturer, was used for running the experiment and integration of area under the peaks.

3.3.3 TAM Results

Preliminary experiments were conducted to determine the repeatability of TAM experiments. Figure 3-4, shows three replicates of the same bulk sample. Typically, three peaks are observed. The first is small and is due to absorption of water vapour into the amorphous lactose (Sebhatu, Angberg, & Ahlneck, 1994). Buckton et al. (1995) show that the type of salt used in the ampoule has an effect on the shape of the initial peak. They suggest the first peak is more complex, including wetting, collapse, change in vapour space and the saturated salt solution. The second peak is high and sharp and represents the crystallisation of lactose. The third peak has been attributed to beta to alpha mutarotation (Briggner, Buckton, Bystrom, & Darcy, 1994). The second peak can be integrated and divided by sample mass. An estimate of amorphicity can then be found when compared with the specific heat of crystallisation (32 J/g) (Sebhatu et al., 1994). In one of the replicates (rep2), the third peak is not clearly separated

from peak two. In this case, the end point of the second peak was estimated and integrated. Table 7 shows that amorphicity ranged from 5.1 to 6.5% for the replicates.

Table 7: Amorphicity results summary for spray dried Supertab

	rep1	rep2	rep3
Mass (g)	0.1046	0.1094	0.1054
Peak area (mJ)	218.29	279	290
Amorphicity (%)	6.5	5.1	5.5

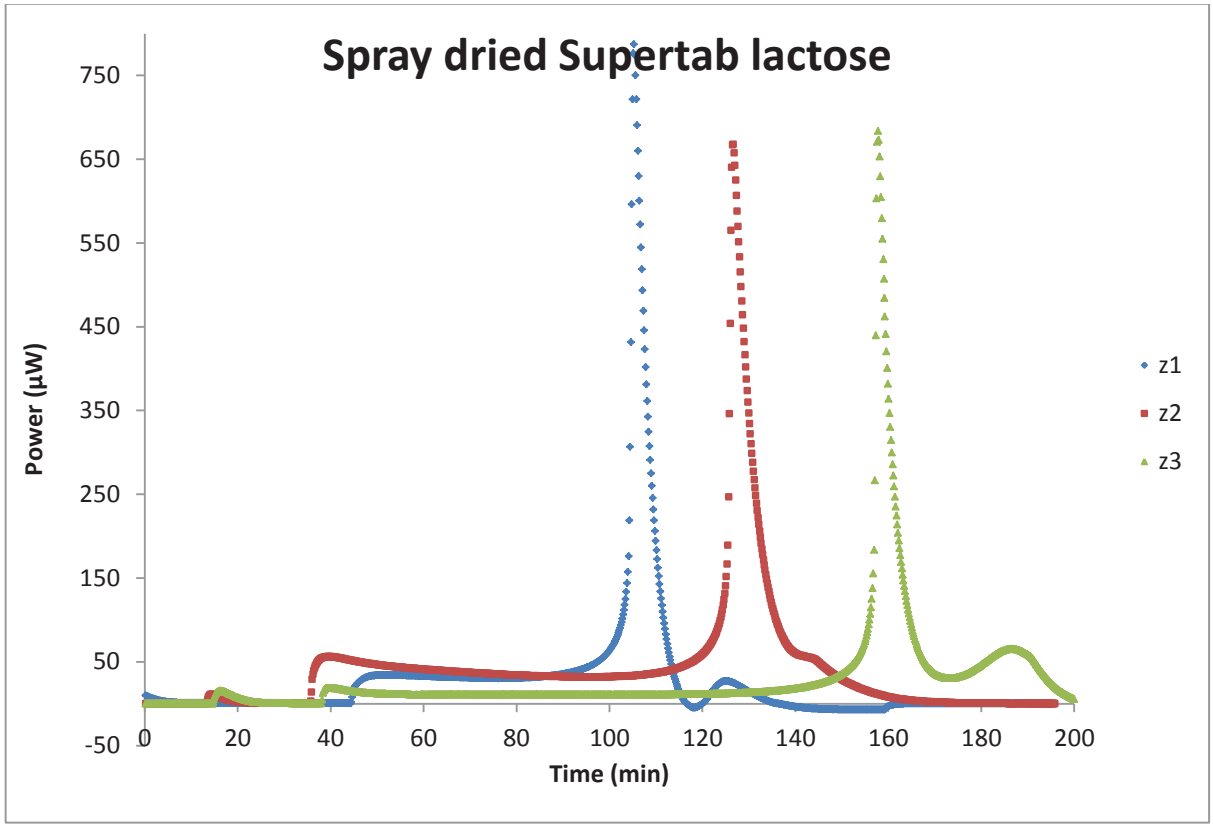

Figure 3-4: TAM results for spray dried Supertab.

The time required for the lactose to absorb the water and crystallise can be reduced by using higher humidity salt solutions (Briggner et al., 1994). Once the water is absorbed the crystallisation is relatively immediate.

Different amounts of amorphous lactose were analysed in the TAM to construct a calibration curve. Both a mix of amorphous and crystalline powder and amorphous only samples were included. The graph of sample mass of amorphous lactose against integrated peak area is

shown in Figure 3-5. A linear regression was carried and prediction intervals calculated are given by the solid and dashed lines, respectively.

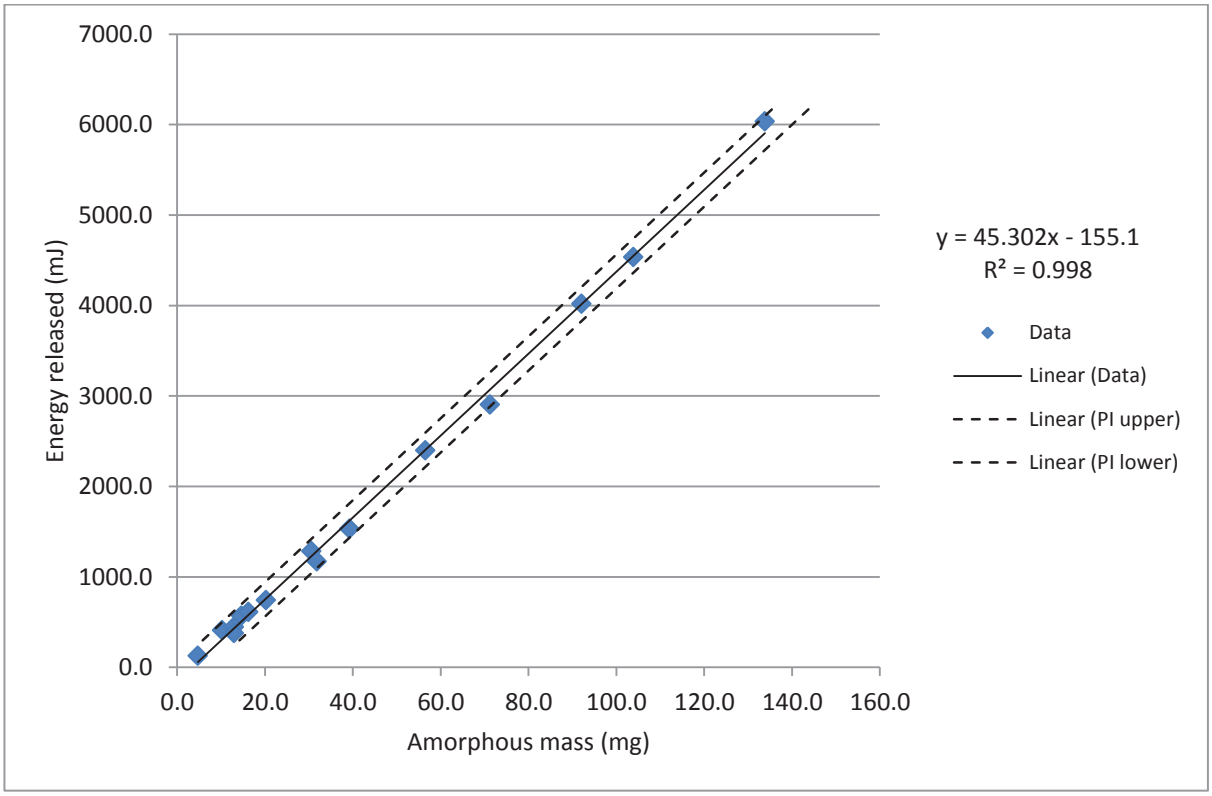

Figure 3-5: Amorphous lactose sample mass against energy released.

The correlation has an R^2 of 0.998. The slope corresponds to a heat of crystallisation of 45.3 J/g. This is within the range of other literature values detailed in Table 8. Differences could be due to where the peak integration is begun and ended. The calibration curve can be used to determine unknown amounts of amorphous lactose from the integrated area.

There was slight evidence of a trend of amorphicity increasing with sample mass (R^2 = 0.44). This could be due to processes other than crystallisation becoming more dominant and increasing peak size as sample mass increases.

Table 8: Enthalpy of crystallisation for amorphous lactose

Reference	J/g	Notes
(Vivoda, Roškar, & Kmetec, 2011)	41.5	Water used - 100% RH
(Buckton, Darcy, Greenleaf, et al., 1995)	45 – 50	20 mg, 80%, 75%, 65%, 54% RH
(Buckton, Darcy, & Mackellar, 1995)	53.9, 58.9	
(Sebhatu et al., 1994)	32	31 mg, 57%, 75%, 84%, 100% RH

3.3.4 Dynamic Vapour Sorption (DVS)

The DVS is a gravimetric based device used to measure moisture sorption. It consists of a balance that a sample holder can be attached and lowered into a controlled humidity chamber. In the instrument, shown in Figure 3-6, the chamber is lowered and the conical mesh sample holder is ready to be removed to add a sample. The mass change is measured as the chamber humidity is altered. To do this the sample is placed into a sample holder then lifted up into the measuring position. The chamber humidity is controlled by changing the mixture of a dry and wet stream of nitrogen gas. A water bath is also attached to help maintain a constant chamber temperature.

The sorption isotherm for amorphous lactose shows that at 30% RH 0.047 grams of water is present for every gram of amorphous lactose. Thus, to measure an amorphicity of 0.1% in 1 g of powder gravimetrically one would need to measure 47 µg of water. At 10% RH this falls to 16 µg of water per gram of powder. Therefore, the required sensitivity for distinguishing between amorphicity of 0.1% is about ± 10 µg water/g powder. Upon calibration with standard weights the maximum error recorded was 26 µg. Therefore, the DVS is sensitive to 0.3% amorphicity.

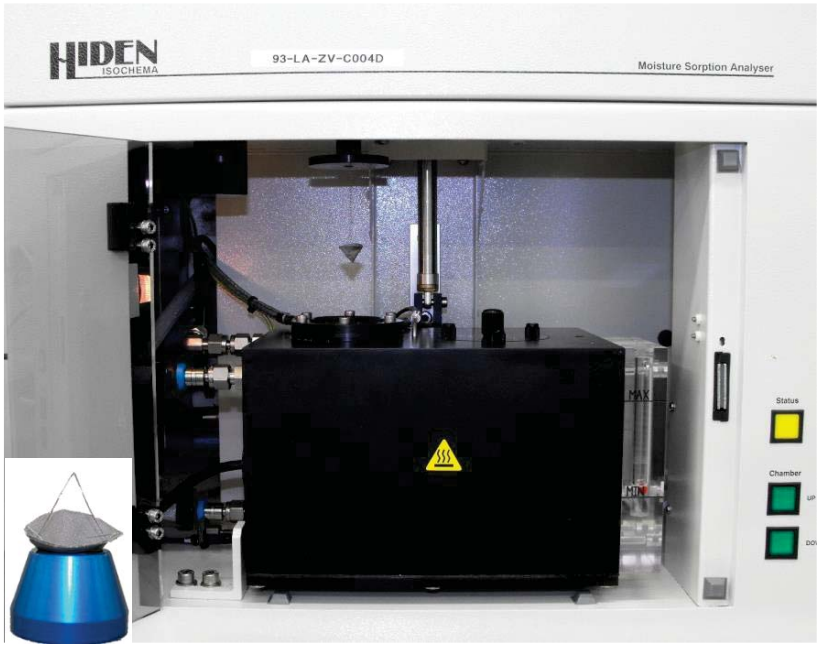

Figure 3-6: HIDEN IGA-Sorp with mesh sample holder visible and chamber lowered. Left: Close up of sample holder.

3.3.5 Method

The isothermal function of IGASorp (DVS software) was used to determine an isotherm for a lactose sample. When doing this the equilibrium mass at a particular humidity is measured. The typical settings used were: sample temperature, 25°C; timeout, 300 minutes; minimum time, 50 minutes; and wait until, 99%. IGASorp estimates the asymptote for sample mass in real time from previous points for a given RH. It gives an estimate of the equilibrium value. The RH values measured at were 0, 0, 10, 20, 30 and 40%. Note that the drying step (0% RH) was typically done for twice as long as the other steps to ensure the sample was sufficiently dried.

The isotherm for amorphous lactose along with experimental data is shown below compared with the GAB model at 25°C (Bronlund & Paterson, 2004). After sample drying for 4 hours, humidity was increased with a timeout of 2 hours at each humidity point.

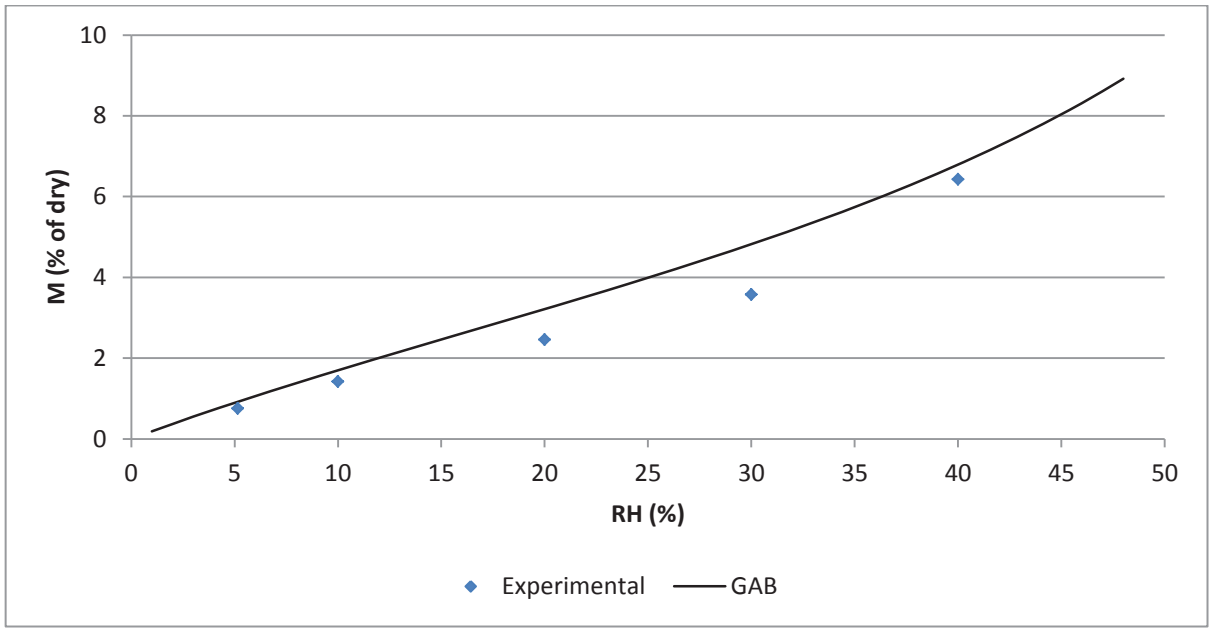

Figure 3-7: Amorphous lactose adsorption isotherm at 25°C.

The isotherm method can be used to determine the amorphicity of a sample containing amorphous lactose. Any isotherm point, or given relative humidity, can be compared with the isotherms for both crystalline and amorphous lactose. The additive isotherm approach of Bronlund (1997) is shown in equation (10).

$$M_{mixture} = (1 - a)\, M_{crystalline} + a\, M_{amorphous} \tag{10}$$

This shows that from the equilibrium content of a lactose mixture, given the equilibrium moisture mass of pure crystalline and amorphous lactose predicted by an isotherm, the amorphous mass fraction (a) of the mixture can be determined.

3.4 Prediction of Crystallisation times

The time required for crystallisation at each set of experimental conditions was predicted using equation (11), given by the Avrami-Bronlund model described in 2.8.3.4 and is a rearranged form of equation (8). The rate constant K_A is given by equation (9) using the constants from Brooks ($C_1 = 3.54 \cdot 10^4$, $C_2 = 110.9$, $C_3 = 2.66 \cdot 10^{27}$).

$$t = \frac{1 - Y}{n_A K_A Y \left(-\frac{\ln Y}{K_A}\right)^{\frac{n_A - 1}{n_A}}} \tag{11}$$

The WLF model given in equation (7) can be rearranged to give crystallisation time using the value of log (t_g) from Roos and Karel (1990).

$$\log t_{cr} = \frac{-17.44\ (T - T_g)}{51.6 + \ (T - T_g)} + 11.14 \qquad (12)$$

The T_g in both these calculations was estimated using the cubic equation given by Brooks (2000), equation (3).

3.5 Control of Experimental Parameters

To measure the crystallisation kinetics it was important to be able to manipulate the T–Tg of the amorphous lactose samples. This can be done by changing the temperature and the humidity conditions. These are both examined below.

3.5.1 Temperature Control

To allow isothermal conditions to be assumed for the experiments the heating rate needs to be at least ten times faster than the reaction rate. Preliminary experiments using borosilicate glass jars showed 5 minutes was needed to heat them. Using the results in Figure 3-8 it can be seen that this limits the upper $T–T_g$ value to about 40°C. The industrial fluidised bed driers being considered in this work have a residence time of around 15 minutes and a $T–T_g$ of up to 56 °C. Use of an aluminium pan reduced the heating time to an average of 140 seconds. This allows $T–T_g$ values of 42°C (t = 26 min) to be measured with the assumption that heating time is negligible. The heating and cooling graphs are shown in Appendix 8.1.2. The effect of $T–T_g$ on crystallisation time is demonstrated by Figure 3-8. Both the Avrami-Bronlund and WLF equation show a strong dependence on $T–T_g$ for crystallisation time. The WLF equation predicts a lower $T–T_g$ for the same crystallisation times.

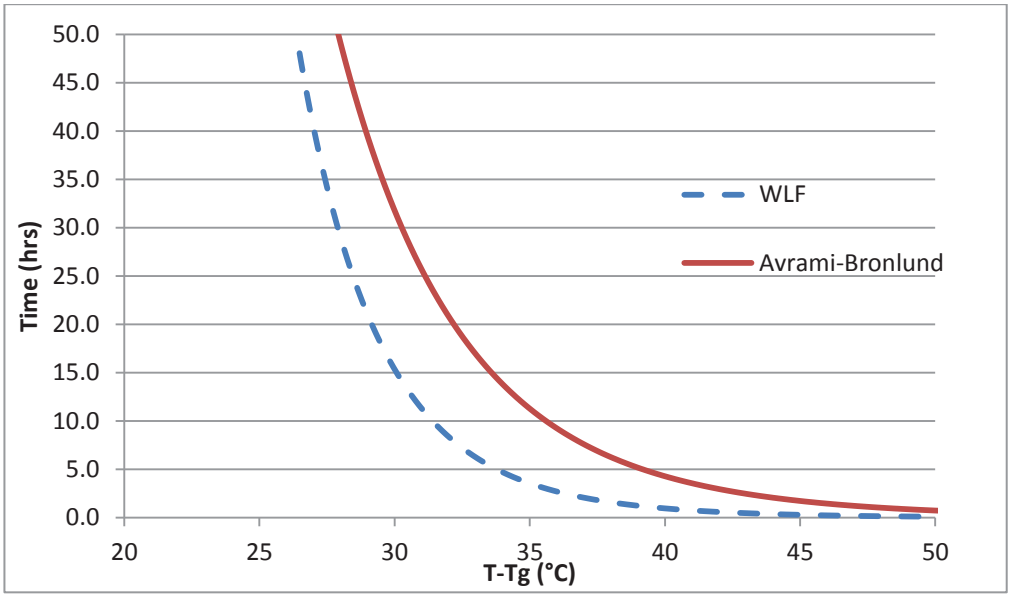

Figure 3-8: Amorphous lactose crystallisation time versus ($T–T_g$).

3.5.2 Humidity

Table 9 shows the T_g calculated from equation (3) at humidity ranging from water activities of 0.05 to 0.55, for temperatures of 4, 20 and 80°C. From this table it can be seen that if each experiment starts at room temperature (20°C) a relative humidity of above approximately 40% RH will cause a positive $T-T_g$ value, creating a potential for crystallisation. This risk can be eliminated if samples are chilled to 4°C, increasing the maximum RH to 55%.

Table 9: $T-T_g$ values at various humidities and temperatures

	T = 4°C		T = 20°C		T = 80°C	
Humidity (a_w)	**T_g**	**$T-T_g$**	**T_g**	**$T-T_g$**	**T_g**	**$T-T_g$**
0.05	82.7	-78.7	82.7	-62.7	82.7	-2.7
0.10	68.8	-64.8	68.8	-48.8	68.8	11.2
0.15	57.4	-53.4	57.4	-37.4	57.4	22.6
0.20	48.0	-44.0	48.0	-28.0	48.0	32.0
0.25	40.3	-36.3	40.3	-20.3	40.3	39.7
0.30	33.9	-29.9	33.9	-13.9	33.9	46.1
0.35	28.4	-24.4	28.4	-8.4	28.4	51.6
0.40	23.3	-19.3	23.3	-3.3	23.3	56.7
0.45	18.3	-14.3	18.3	1.7	18.3	61.7
0.50	13.0	-9.0	13.0	7.0	13.0	67.0
0.55	6.9	-2.9	6.9	13.1	6.9	73.1

Salt solutions can be used to create different relative humidity conditions. When used as saturated solutions they also offer the advantage that any moisture released during crystallisation is drawn into the solution. Figure 3-9 shows humidities for different saturated salt solutions, it can be seen that many of these have varying humidity with temperature. In this work Magnesium chloride and Lithium chloride were selected for use. These two salts cover the humidity range required and their relative humidity remains almost stable over the temperature range of interest. The crystallisation time using Avrami kinetics was calculated using the different saturated salt solution humidity values from Greenspan (1977). Taking into account the uncertainty values given in the literature, errors of 31-53% and 5-16% for LiCl and $MgCl_2$, respectively, could be introduced. Thus, direct measurement of humidity is desired.

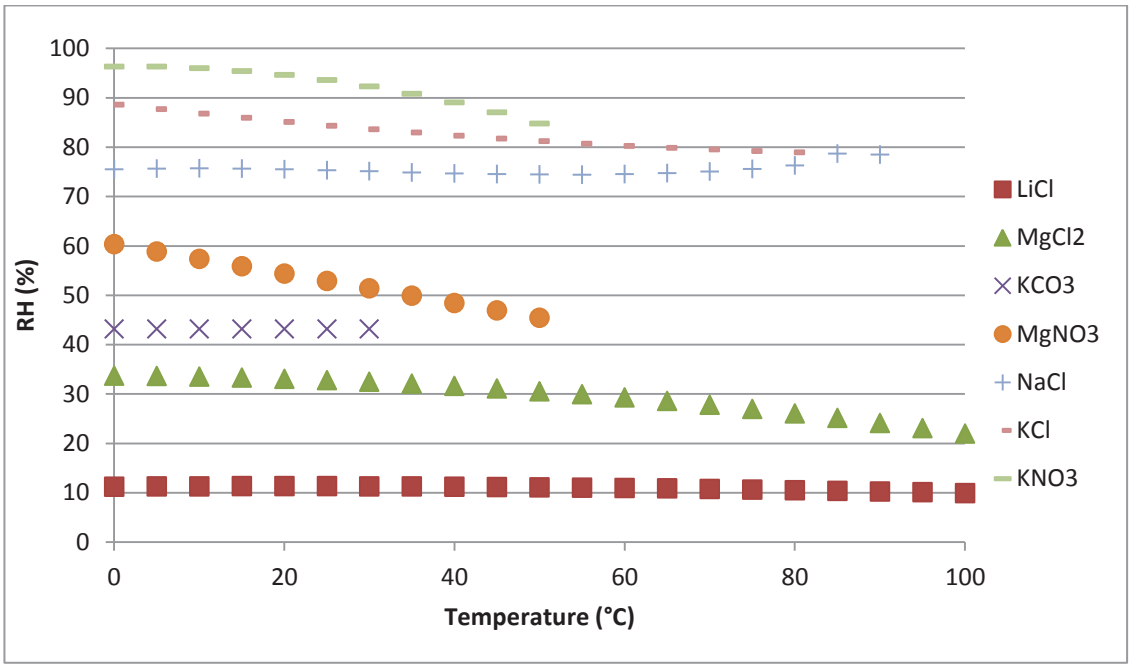

Figure 3-9: Salt range and stability (Greenspan, 1977).

DS1923-F5# Ibuttons manufactured by Maxim Integrated were used to provide additional information on the humidity and temperature in the sealed containers. These are small self-contained, data logging sensors that can measure both temperature and humidity. The operating limits are below ~85°C and 40% RH.

Figure 3-10 below shows the required temperatures for various $T–T_g$ conditions and associated crystallisation times for the two salts.

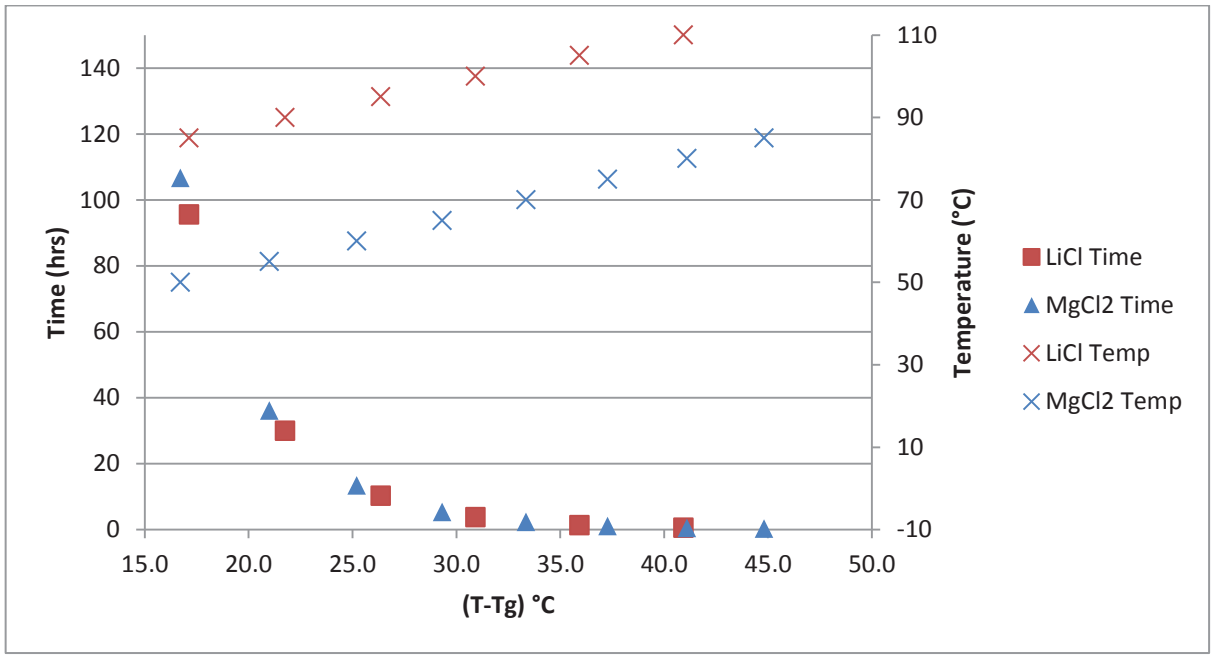

Figure 3-10: LiCl and MgCl2 salt solution temperatures and crystallisation times for various T–T_g.

From Figure 3-10 is can be seen that to achieve a T–T_g of ~35°C a temperature of 72°C and 105°C for $MgCl_2$ (27% RH) and LiCl (10% RH) respectively, is required. Not considered in this graph is that $MgCl_2$ salt at room temperature (33% RH) is quite different to that at the experimental temperatures (25-31% RH), and thus, there will be time required for equilibration. Also not considered is the effect of the water released during crystallisation. Though this should be absorbed by the salt, the availability of any additional water will cause an inflated reaction rate.

3.6 Experimental Procedure

For each of the amorphous lactose crystallisation measurements the following procedure was followed. A controlled humidity box was used for sample preparation. The humidity was controlled by passing the air though a column of Drierite (anhydrous calcium sulphate). Fresh desiccant was regularly added to the column to prevent it becoming exhausted. The relative humidity (RH) was set to 30% RH and the dehumidification process begun. The dehumidification process took approximately one hour.

The steel sample pans, lids, screws, saturated salt solution and associated utensils were placed in the chamber and allowed to equilibrate. The lowered RH ensured that the setup process occurred below T_g so that no crystallisation occurred.

A small amount of amorphous lactose was then spooned into a 300 µm sieve. A brush was used to spread the lactose through the sieve. The pan was weighed to ensure around 0.1 g of amorphous lactose was in the pan.

The saturated salt was prepared by adding 3 g of solid salt to a thin, rounded plastic container. Saturated salt solution was then pipetted into the container until the container was almost full. As well as providing a large surface area for mass transfer, this ensured the salt solution was saturated and would remain so at higher temperatures. A small piece of bluetak helped the container to adhere to the sample pan.

An activated ibutton, facing upwards, capable of measuring relative humidity and temperature, was also added to the pan. Figure 3-11 shows the pan setup prior to the sealing process.

Grease was added to the rubber o-ring and the lid pressed firmly down to help create an airtight seal. Four screws were then tightened to further seal the pan. This was repeated for each pan.

The pans were left for 14 hours to allow the salt solution and the amorphous lactose particles to reach the equilibrium humidity expected inside the pan. Ibutton readings from preliminary experiments were used to determine the time required for equilibrium.

The pans were then placed into a water bath at the desired temperature. In some cases pans were stacked with one on top of another. The time each pan was held at temperature was calculated from the crystallisation model and the crystallinity expected.

After the calculated amount of time, the pans were removed and placed into another water bath 2°C above the calculated dew point. The dew point was calculated using ITS-90 constants (0-100°C) for the saturation pressure, enhancement factor and dew point (Hardy, 1998). Cooling was staged to allow moisture to absorb back into the salt solution and prevent condensation during cooling. The cooling stage ensures that the dew point is not breached and that there is enough time for equilibrium humidity to be reached at the lowered temperature.

After 45 minutes, the pans were then placed into cooler water, at least 2°C above the dew point. After 45 minutes in cool water the pans were removed and they were ready for analysis.

Pending analysis, samples were stored over phosphorous pentoxide to prevent further crystallisation.

Figure 3-11: Sample pan with saturated salt solution and ibutton (bottom).

3.7 Conclusion

The kinetics of amorphous lactose investigated with reference to the conditions at the industrial lactose plants. The mass balance showed that more drying occurred in the flash dryer at Plant A than at Plant B, and vice versa for the fluidised bed. An estimate of the $T-T_g$ at Plant A was much lower than at Plant B indicating it is more likely that amorphous lactose will remain after the Plant A drying process. The experimental method selected was a sealed vessel containing amorphous lactose and saturated salt solution that is first equilibrated, and then exposed to temperatures above T_g. Subsequent measurement of amorphicity by TAM and DVS will be used for measurement of kinetics. The next chapter focuses on measuring the diffusivity of water through amorphous lactose particles which is important for measuring the equilibrium time.

4 Diffusivity

4.1 Method

The DVS was used to measure mass change due to water adsorption. The sequence mode of the software was used in order to record mass as a function of time. The sample was first dried then humidity was increased to 30-40% RH for a minimum of 4 hours. The amount of time required for drying and equilibration varied with the type of lactose used. The mass and time data was then converted to a fraction of accomplished change (Y_{ac}) using the dry mass and equilibrium mass.

The situation was modelled as unsteady state diffusion into a sphere. The solution to the total amount of diffusing substance entering or leaving the sphere is given by Crank (1956), equation (13). Where, C_o, C_i and C_f are the bulk, initial and final concentrations, respectively. The solution assumes a constant surface concentration equal to the equilibrium value. In the small lactose particles the surface moisture content is unlikely to reach the equilibrium value, introducing error into the results when using this solution.

$$Y_{ac} = \frac{C - C_i}{C_f - C_i}\,, \qquad Y_{tot} = 1 - \frac{6}{\pi^2}\sum_{n=1}^{\infty}\frac{1}{n^2}\,\mathrm{e}^{-n^2\pi^2 F_o} \tag{13}$$

F_o is the Fourier number.

$$F_o = \frac{Dt}{R^2} \tag{14}$$

The user defined function created in Microsoft Excel to calculate the summation in equation (13) for an absolute radius value, Y_{tot}, is shown in Appendix 8.3.1. Y_{tot} is the total amount of diffusing substance entering or leaving the sphere. This was compared with the Y_{tot} calculated by taking into account the particle size distribution of amorphous lactose (Y_{totpz} Appendix 8.3.2). The particle size distribution was measured by a Malvern Mastersizer 2000 using Propan-2-ol as the dispersant. The experimental fractional change (Y_{exp}) was found by calculating the weight loss at each time as a fraction of the total mass loss. By minimising the

sum of squares between the experimental and model values the diffusivity of water through lactose was estimated.

4.2 Results

Above the glass transition the reduction in viscosity allows sorption rates to increase. The Brooks (2000) cubic equation calculated a T_g of 33.9°C at 30% RH (see Table 9). For a temperature of 25°C a positive $T-T_g$ is only reached at 38% RH. Thus, diffusivities calculated from a start-end RH below 38% RH should be similar. The adsorption curve for spray dried Supertab, for two passes with a humidity increase from 0% to 35% RH, is shown in Figure 4-1. The dry and end weights for each pass were very similar. The higher diffusivity value for the second pass of the Supertab sample suggests that the glass transition has already begun, causing an increase in molecular mobility. Figure 4-2 shows a similar experiment for spray dried amorphous lactose with a humidity increase from 0% to 20% RH. The glass transition should not be a factor at this humidity. However, the calculated diffusivity is larger for the second pass. Inspection of the dry and end weights shows a 2.7% and 0.07% mass difference, respectively. Insufficient drying after the first pass could explain why the second pass was quicker to reach equilibrium.

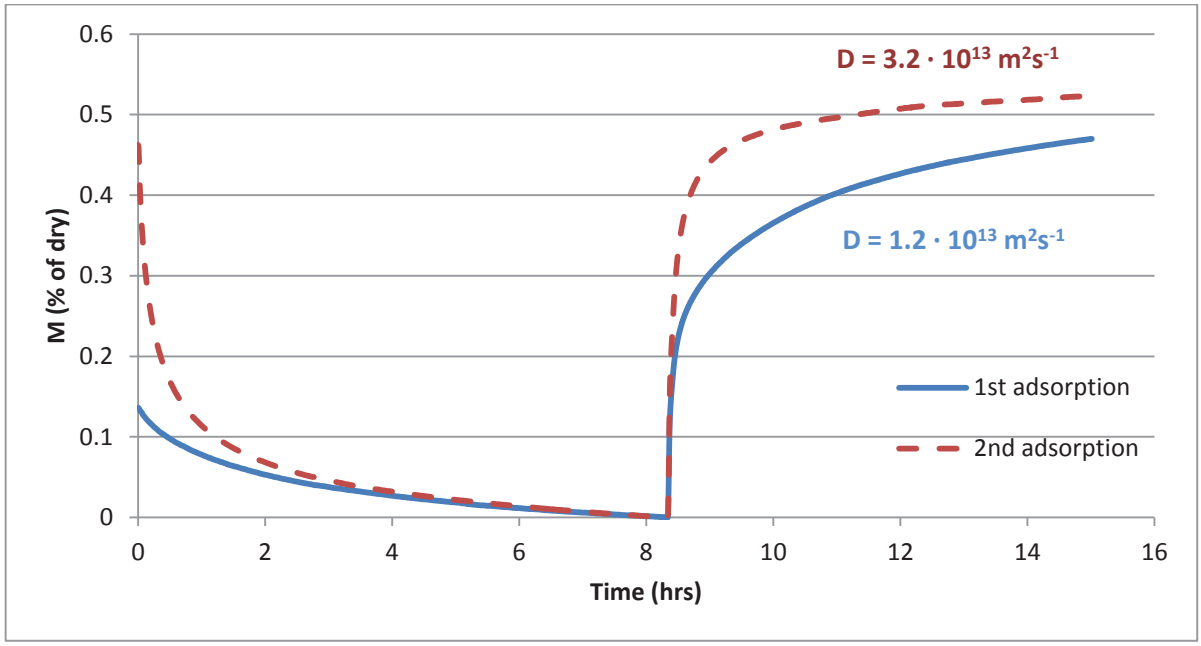

Figure 4-1: Supertab adsorption for 2 passes with RH increased from 0 to 35%.

Experimental data (Y_{exp}) for a single adsorption pass is plotted against the two models (Y_{tot} and Y_{totPZ}) in Figure 4-3 and Figure 4-4. The Y_{tot} gave the lowest error, with a diffusivity of $4.4 \cdot 10^{-15}$ m^2s^{-1} and $8.3 \cdot 10^{-12}$ m^2s^{-1} for spray dried and freeze dried lactose respectively.

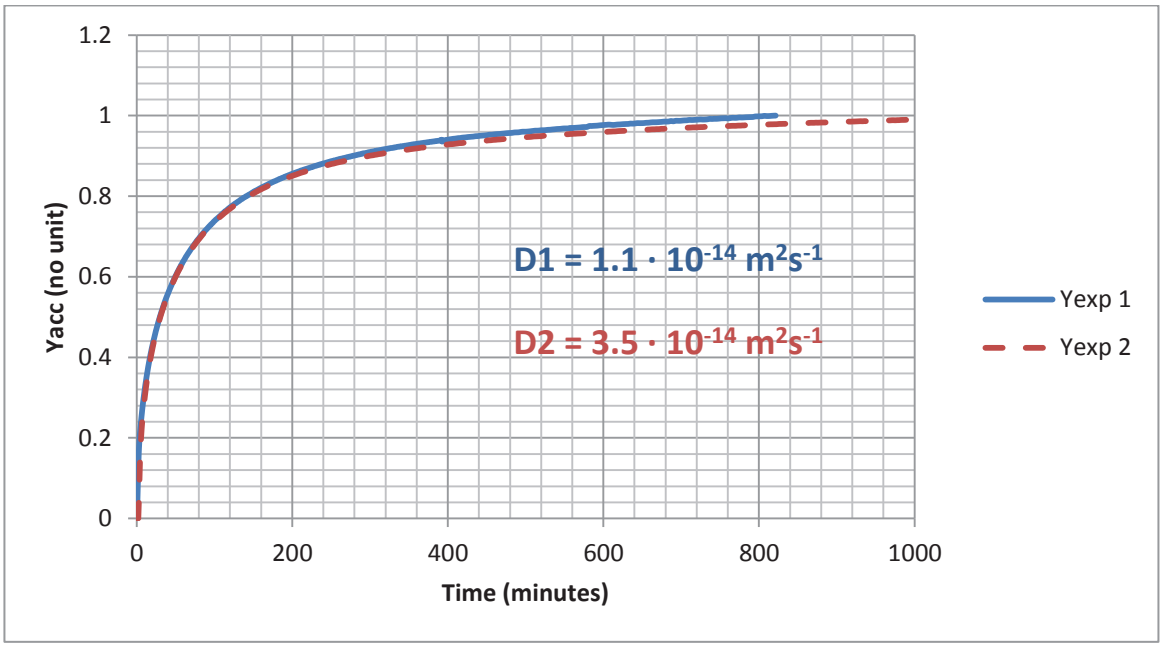

Figure 4-2: Y_{exp} for amorphous lactose sample from 0 to 25% RH, 2 runs, Y_{pztot} given for diffusivity.

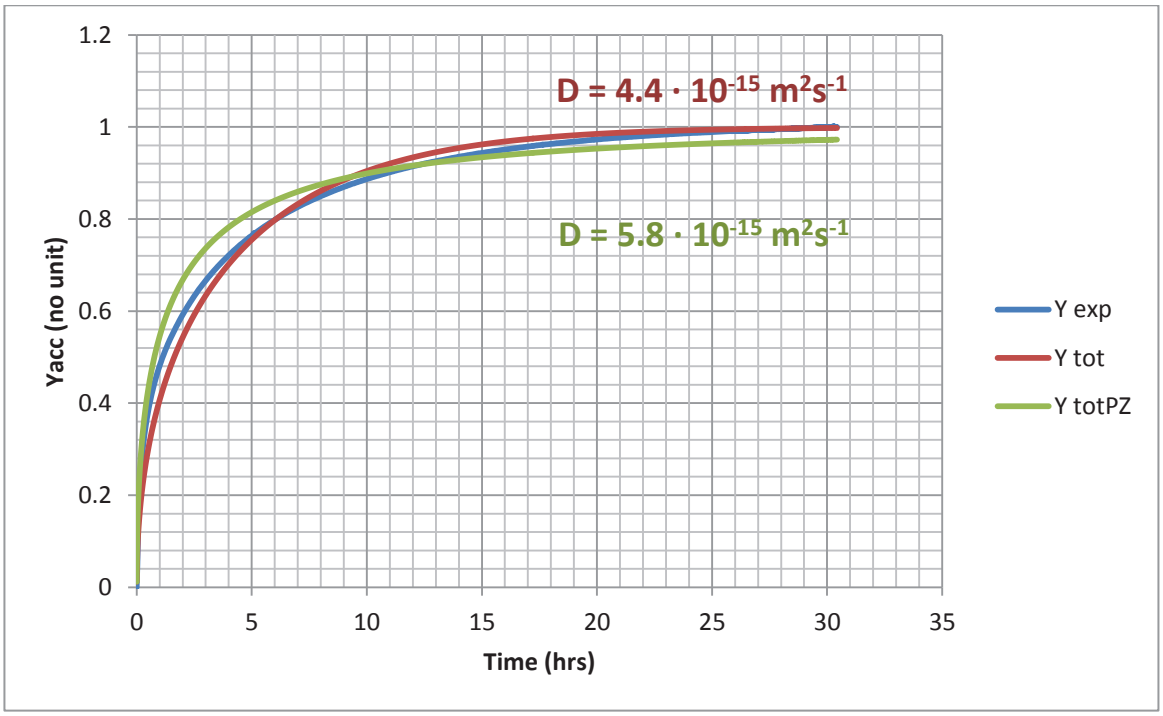

Figure 4-3: Fitted model to experimental data for fractional accomplished diffusion change out of a spray dried lactose dried for 16 hours then subjected to 30% RH.

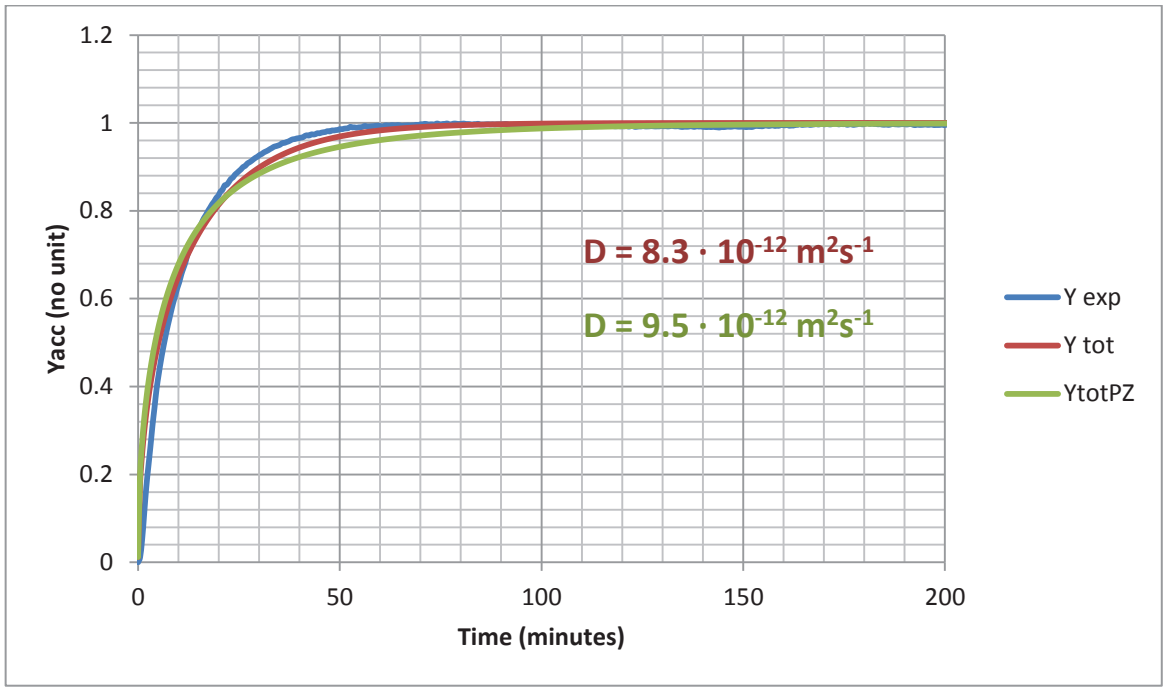

Figure 4-4: Fitted model to experimental data for fractional accomplished diffusion change out of a freeze dried lactose sphere dried for 10 hours then subjected to 35% RH.

Table 10 below shows the fitted diffusivities with the associated humidity start and end points used in the DVS.

Table 10: Summary of diffusivities of different lactose types

Supertab		Spray dried		Freeze dried		Milled	
Start-end RH	Diffusivity (m^2/s)	Start-end RH	Diffusivity (m^2/s)	Start-end RH	Diffusivity (m^2/s)	Start-end RH	Diffusivity (m^2/s)
0-40%	4.9E-13	0-45%	1.2E-14	0-40%	8.3E-12	20-30%	5.2E-14
0-40%	4.1E-13	0-40%	1.1E-14	0-35%	6.3E-12	0-35%	3.7E-13
0-40%	2.3E-13	0-40%	7.7E-15	0-35%	8.3E-12	0-35%	6.1E-13
0-35%	1.2E-13	0-35%	5.3E-15			0-30%	4.0E-13
0-35%*	3.2E-13	0-35%	3.8E-14				
0-35%	6.7E-13	0-30%	4.4E-15				
0-30%	1.7E-13	0-30%	2.6E-15				
		0-20%	1.1E-14				
		0-20%*	3.5E-14				
Average	3.4E-13	Average	1.4E-14	Average	7.6E-12	Average	3.6E-13

**Same sample as row above*

Figure 4-1 suggested structural change of the partially amorphous lactose occurred after one pass with humidity treatment to 30%. If a significant glass transition effect was present the diffusivities fitted with end points above and below 30% RH should be different. A statistical comparison for spray dried lactose between the diffusivity values found with an endpoint over 30% RH, to those with an endpoint 30% RH and below, was conducted. There was no evidence for a difference between the means (P = 0.876). The diffusivities values for Supertab and milled lactose for the low endpoint RH were also within the range of the other diffusivity values found. Thus, the diffusivity values determined with end RH values above 30% RH were judged valid and were included in the calculated average.

Averaging over the appropriate ranges, diffusivities of $3.4 \cdot 10^{-13}$, $1.4 \cdot 10^{-14}$, $7.6 \cdot 10^{-12}$ and $3.6 \cdot 10^{-13}$ m^2s^{-1} were obtained for Supertab, spray dried, freeze dried and milled lactose, respectively. For spray dried amorphous lactose the calculated diffusivity takes 4.2 and 15.7 hours to reach 90% and 95% total moisture change. Thus, the allowed time of 14 hours was deemed sufficient for enough of the lactose to equilibrate with the RH of the pans used.

A t-test was carried out between each lactose type to determine the probability of how far apart the means would be if the null hypothesis of equal means held, assuming independent unequal variance. With an alpha level of 0.05, there is no evidence for a difference between means for the Supertab-Milled and Spray dried-Milled comparisons. Because these powders were produced on a spray dryer this is not surprising.

Table 11: T-test between lactose types

Comparison	Probability
Supertab-Spray Dried	0.004*
Supertab-Freeze Dried	0.008*
Supertab-Milled	0.924
Spray dried-Freeze dried	0.008*
Spray dried-Milled	0.058
Freeze dried-Milled	0.007*

**Below α=0.05, null hypothesis rejected*

Ripberger (2010) found a diffusivity of $3.41 \cdot 10^{-14}$ and $4.48 \cdot 10^{-11}$ m^2s^{-1} for spray dried and freeze dried lactose respectively. Bronlund (1997) found a value $2.33 \cdot 10^{-14}$ m^2s^{-1} for spray dried amorphous lactose. The trend of a much higher diffusivity for freeze dried over spray dried lactose is confirmed. The difference is due to the fact spray dried lactose shrinks during the removal of water, while freeze dried lactose does not shrink during lyophilisation, resulting in a more porous particle (Ripberger, 2010; Vollenbroek et al., 2010). Additionally, for freeze

dried lactose, the low temperatures of the freezing process hinder lactose-lactose interactions giving a higher free volume and therefore, more reliance on the much higher diffusivity of water in air ($2.6 \cdot 10^{-5}$ m^2s^{-1} at 25°C).

The results for freeze dried lactose are roughly an order of magnitude smaller than those Ripberger reported. The DVS takes approximately 90 seconds to reach the required humidity. With a diffusivity of $4.48 \cdot 10^{-11}$ m^2s^{-1} we would expect 61% of the accomplished change to be complete after 90 seconds. The DVS ramp rate may be limiting the rapid adsorption of freeze dried lactose leading to an underestimation of diffusivity. The average result of $1.4 \cdot 10^{-14}$ m^2s^{-1} for spray dried amorphous lactose was slightly lower than the values reported in the literature. Given the variation between replicates this can be put down to experimental error.

The milled lactose results were expected to be similar to those of spray dried amorphous lactose. The t-test results showed there was no evidence for a difference between the means of the milled lactose and Supertab or spray dried lactose. In particular there was very similar diffusivities for Supertab and milled lactose with $3.4 \cdot 10^{-13}$ and $3.6 \cdot 10^{-13}$ m^2s^{-1} respectively. This close agreement is unusual given their different structures. Supertab contains around 5-12% spray dried amorphous lactose localised to the centre of the particle, while, milled lactose has a thin amorphous surface layer.

Figure 4-5 below shows sample of amorphous lactose dried, then exposed to 30%, and later 50% RH. After 12 hours at 30% RH, 91% of the moisture change has been achieved. The adsorption rate is slow to start ($D = 4.4 \cdot 10^{-15}$ m^2s^{-1}) then rapidly increases once the RH is increased to 50%. The graph is consistent with a change in molecular mobility above a certain point (T_g) giving an increased adsorption rate. This allows the sample to crystallise, and water is released. The rapid adsorption and desorption is indicative of a catastrophic crystallisation event. Comparing with Figure 2-7 there exists a period of lag between the humidity increase and the first point of mass loss (onset time). However, at 2.2 and 4.6 hours this is much lower than the approximately 15 hours predicted by Burnett (2006). The period of equilibrium at 30% RH is likely to have lowered the required induction or onset time. This DVS crystallisation method could be used to determine the minimum humidity required for crystallisation to occur.

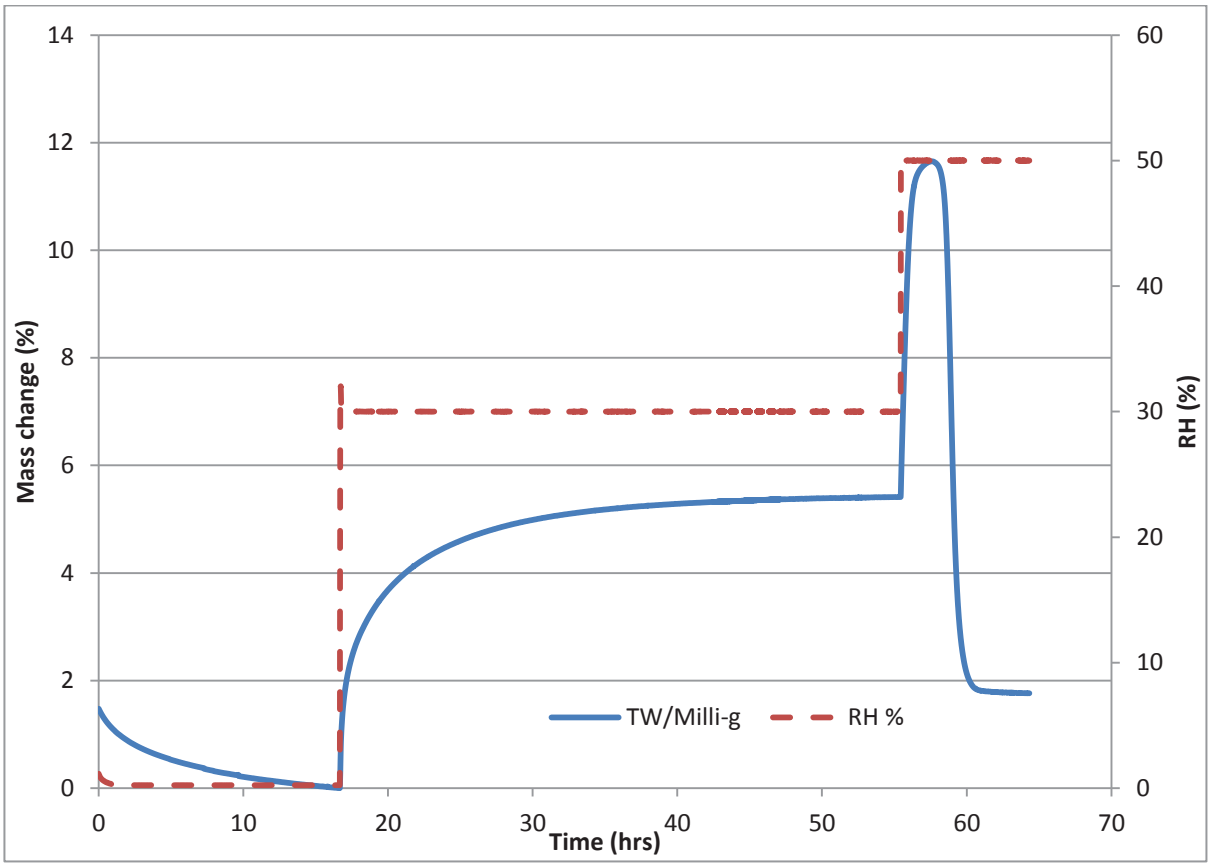

Figure 4-5: Crystallisation of spray dried amorphous lactose at 50% RH and 25°C.

4.3 Conclusion

Diffusivities of $3.4 \cdot 10^{-13}$, $1.4 \cdot 10^{-14}$, $7.6 \cdot 10^{-12}$ and $3.6 \cdot 10^{-13}$ m^2s^{-1} were found for Supertab, spray dried, freeze dried and milled lactose, respectively. A t-test showed no evidence for a difference between means for the Supertab-Milled and Spray dried-Milled sample comparisons. As these powders are produced in a spray drier this is not surprising. The literature trend of much higher diffusivities for freeze dried compared with spray dried lactose was followed. The freeze dried diffusivity values were lower than other literature values, but this may be due to the DVS ramp time. From the determined diffusivity, after 9.9 hours, 95% of the moisture change was achieved in amorphous lactose particles showing the time allowed for the amorphous lactose in the samples to equilibrate was sufficient. The crystallisation kinetics results are discussed in the next chapter.

5 Amorphous lactose crystallisation kinetics

5.1 Milled lactose

A sample of milled lactose was taken from the plant and tested for amorphous content. Due to the melting and rapid cooling of the milling process it was expected a thin layer of amorphous lactose will be produced. The expected amorphous content was around 1%, giving a chance to test the sensitivity of the analytical techniques.

Figure 5-1 shows the DVS data for unconditioned and conditioned milled lactose plotted with the GAB crystalline isotherm (Bronlund & Paterson, 2004). The milled lactose was conditioned by exposing to a RH above 60% for 24 hours. The conditioned lactose closely follows the model showing it was fully crystalline. The average amorphous level in the unconditioned milled lactose was calculated by using equation (10) as (1.1 ± 0.4) % (error = 2 x SD). The DVS is able to distinguish well between the low amorphicity milled samples.

In contrast, analysis using the TAM was less clear. There was no clear crystallisation peak for both milled and milled conditioned. It is possible the crystallisation peak was obscured by the primary adsorption peak. From this it is concluded, the TAM is not as well suited as the DVS to detecting low levels of amorphous lactose found in milled lactose.

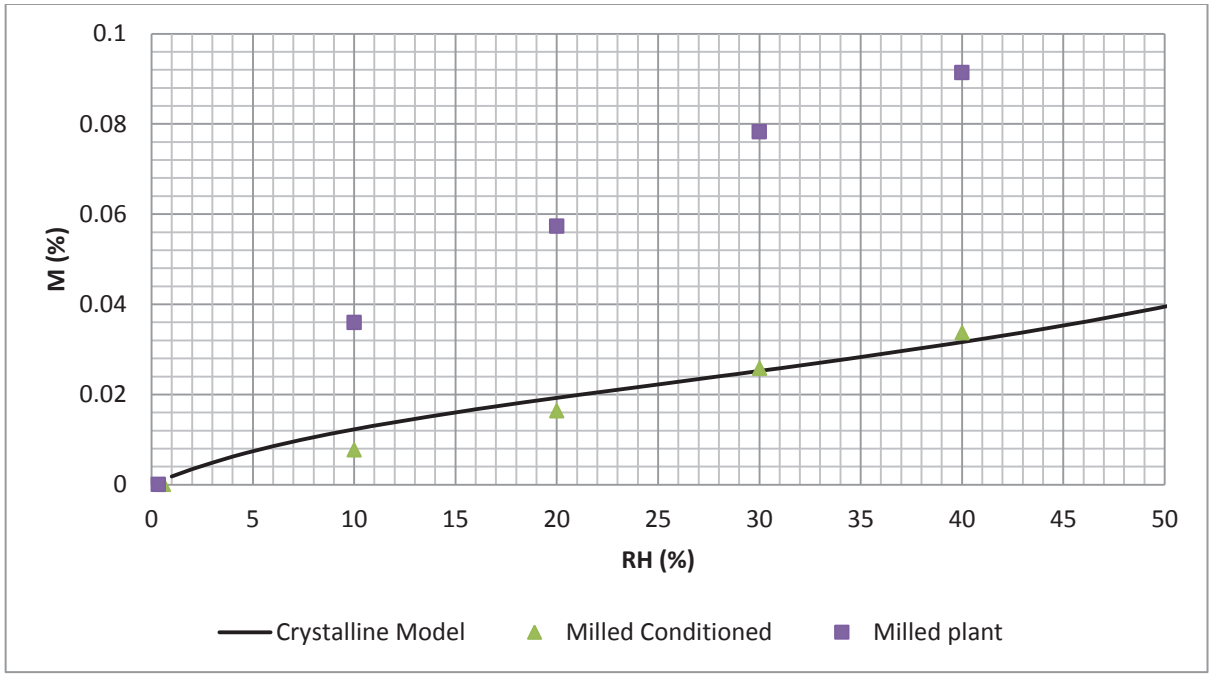

Figure 5-1: Lactose isotherms for crystalline, milled and milled conditioned lactose.

5.2 Amorphous Lactose

5.2.1 Variable $T-T_g$

Spray dried lactose prepared via section 3.2.2 was exposed to temperatures above the predicted glass transition using the method described in section 3.6. The time at which samples were exposed to the specified temperature, was held constant at 1.6 hours and the temperature increased. Trials were carried out at 57.7, 62.7, 67.7, 70 and 72.5°C.

The amorphicity results, as determined by TAM, of trials over the range of $T-T_g$ are shown in Figure 5-2. At a $T-T_g$ of 31.6°C one of the three replicate pans showed no evidence of amorphicity. Pans treated at above this at a $T-T_g$ of 33.4°C and 35.3°C also showed no evidence of amorphicity. The results indicated that the lactose was either completely amorphous or completely crystalline, when a $T-T_g$ of above 31.6°C was used for 1.6 hours. Samples at a $T-T_g$ below 31.6°C were completely amorphous. Freeze dried lactose also showed no evidence of amorphicity at a $T-T_g$ of 33.4°C after 1.6 hours.

The sharp transition illustrated by the experimental data was in contrast to the more gradual reduction in amorphicity predicted by the Avrami-Bronlund model. The Avrami-Bronlund model predicted an amorphicity of 50% at a $T-T_g$ of 28.4°C. The WLF equation predicted a $T-T_g$ of 38°C before crystallisation occurred. Crystallisation occurred at a lower $T-T_g$ than predicted by the WLF equation. These results suggest that crystallisation is an all or nothing effect, if it begins it continues to completion. They lend some support to the WLF equation which does not contain crystallinity as function of crystallisation time.

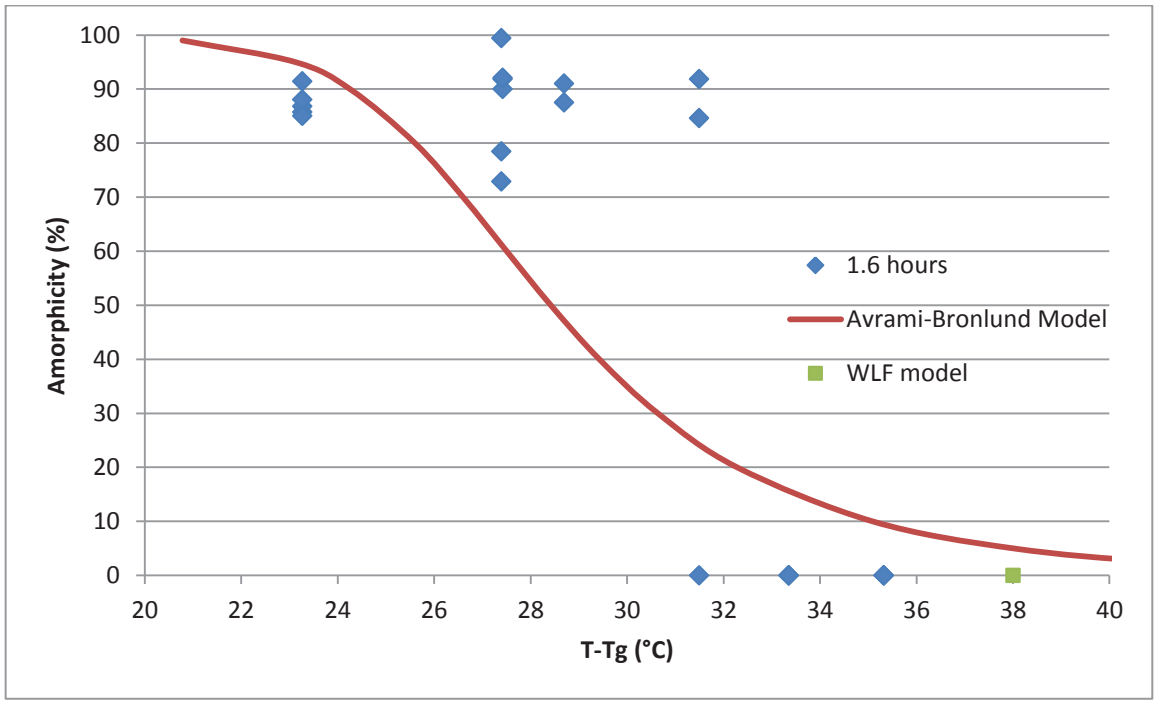

Figure 5-2: Experimental $T-T_g$ against amorphicity data after 100 minutes including model predictions.

5.2.2 Constant $T-T_g$

Experiments using the method in section 3.6 were conducted using spray dried amorphous lactose. It was attempted to create an amorphicity against time graph using a constant temperature (and thus $T-T_g$) of 57.7°C ($T-T_g$ = 23.3°C). At this $T-T_g$, estimations from the Avrami-Bronlund models for 1% and 90% amorphicity ranged from 2.0 to 143.8 hours. The WLF equation predicted a crystallisation time of 148 hours. Experiments were run for 1.6, 3.1, 6.3, 12, 14.5, 15.5, 21, 30, 79 and 96 hours at a constant temperature (57.7°C).

Figure 5-3 below shows the amorphicity determined by the TAM against the time exposed to a $T-T_g$ of 23.3°C. Note that there is overlap of points at the high and zero amorphous level giving the impression of more data spread than is the case. There is no sign of crystallisation until 12 hours, when 2 of the 8 replicate pans sampled showed some evidence of crystallisation. At 15.5 and 16.5 hours one each of two replicate pans treated showed no evidence of amorphicity with the other showing some evidence of amorphicity. All pans treated for 21 hours or longer ($T-T_g$ > 30°C not graphed) showed no evidence of amorphicity, suggesting complete crystallisation had occurred.

The constant $T-T_g$ results further advocate that crystallisation is an all or nothing event. The fact that some replicate pans crystallised and some did not, with few between, also showed that crystallisation was rapid. The proposed method relied on the ability to halt the

crystallisation reaction somewhere between fully amorphous and fully crystalline lactose. Due to the lack of repeatable values in this range using this method to obtain kinetic data is unviable.

The rapid crystallisation could be due to an autocatalytic effect from moisture release during crystallisation. Another explanation is a showering event, sudden formation of many small crystals, as often seen in supersaturated lactose solutions. Experiments detailed in section 5.2.3 were carried out attempting to elicit whether there was evidence for a showering event.

The transition was more defined in the constant time case compared with the constant $T-T_g$ case. As a shorter exposure time was used, a higher $T-T_g$ was necessary to achieve crystallisation in the variable $T-T_g$ case; thus, there were not a small number of pans that were in between (located in the 10 to 70% amorphous range).

Overall, the results show that a small change in $T-T_g$ or time can lead to amorphous lactose crystallising. This means, only a small change in fluidised bed temperature or residence time may be required in order to completely crystallise lactose and prevent any downstream problems.

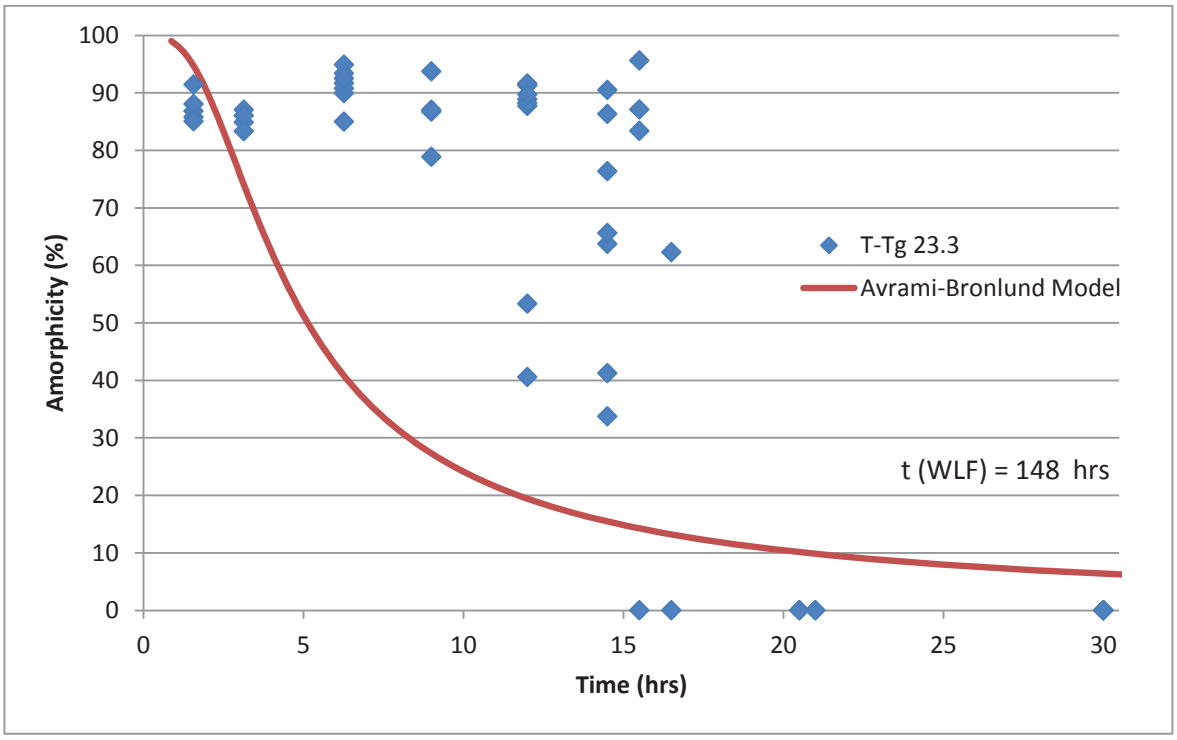

Figure 5-3: Experimental data at $T-T_g$ of 23.3°C against amorphicity for spray dried lactose including model predictions.

5.2.3 Supertab

The aim of experiments using Supertab was to investigate the showering as a dominant cause of the rapid crystallisation described above. Supertab is spray dried lactose containing 5-12% amorphous lactose. Due to Supertab's high flowability it is likely the amorphous is located near the centre of the lactose particle. If showering was significant, it was thought that the crystalline surface would have a seeding effect on the amorphous contents. By providing nuclei for crystals to grow, crystallisation might occur at a lower temperature than with pure amorphous lactose.

The Supertab used was SuperTab™ 11SD manufactured for DMV-Fonterra Excipients. The standard was found to range from 6.6% to 9% amorphous using the TAM method and 6.4% to 6.7% using the DVS method. The DVS was mainly used for analysis because it showed better repeatability for the Supertab standard and it was previously shown to be sensitive at lower amorphicities.

Supertab treated for 2 hours at 80% RH, and shown to have no amorphous content via the TAM, showed a result in the DVS. The DVS analysed samples varied widely from the typical isotherm and were predicted to contain an amorphous lactose content ranging from 1.3% to 3.4%. This is likely due to the method of amorphicity determination relying on adsorption isotherms and the structure of Supertab allowing it to absorb more water through capillary condensation than normal crystalline lactose. This effect makes it difficult to quantitatively assess the amorphicity of Supertab using the DVS.

Supertab treated for 100 minutes at a $T-T_g$ of 25.2°C showed no evidence of amorphicity when taking into account TAM and DVS results. This was below the $T-T_g$ of 31.5°C at the same exposure time required for spray dried amorphous lactose to crystallise. At a $T-T_g$ of even lower, 23.3°C, there was also no evidence of amorphicity. When treated for 69 and 93 hours at a $T-T_g$ of 16°C there was also no evidence of amorphicity. These results suggest a seeding effect as crystallisation occurs at a much lower $T-T_g$ than with completely amorphous lactose. Thus, there is some support for rapid crystallisation due to a showering event hypothesis.

5.3 Conclusion

The DVS was better suited to measuring the low amorphicity of milled lactose than the TAM. The freshly milled lactose was found to have an amorphicity of (1.1 ± 0.4) %.

Variable and constant $T-T_g$ results were found using spray dried amorphous lactose. At a variable $T-T_g$ the experimental data crystallised at a $T-T_g$ of 33.4°C compared with the 38°C predicted by the WLF equation. For a $T-T_g$ of 23.3°C there was no evidence of crystallisation until after 12 hours. Both the variable and constant $T-T_g$ results using fully amorphous lactose showed that crystallisation was rapid. This contrasted with the gradual transition predicted by the Avrami-Bronlund model. The rapid crystallisation observed means a small change in the temperature or humidity conditions of a fluidised bed dryer could cause crystallisation to occur or cease occurring.

Two main explanations for rapid crystallisation were considered; an autocatalytic effect due to moisture release during crystallisation, or a showering event as often seen in supersaturated lactose solutions. Experiments conducted using partially amorphous lactose, Supertab, indicated a seeding effect, adding support for the cause of rapid crystallisation due to a showering event.

6 Conclusions and Suggestions for Future Work

The glass transition temperature was identified as an important characteristic of amorphous lactose and its kinetics. The quantity $T-T_g$ is part of the WLF and Avrami equations used to model crystallisation.

The diffusivity through water of several lactose types were investigated using the DVS. The diffusivity through water of spray dried amorphous lactose was found to be $1.4 \cdot 10^{-14}$ m^2s^{-1}, slightly lower than that found in earlier work. For freeze dried lactose the diffusivity was $7.6 \cdot 10^{-12}$ m^2s^{-1}, lower than earlier work, but this may be due to the humidity ramping limitations of the DVS. The rate of moisture sorption of amorphous lactose was shown to dramatically change once above a certain point, before crystallisation occurred. The diffusivity through water of Supertab and milled lactose was shown to be $3.4 \cdot 10^{-13}$ m^2s^{-1} and $3.6 \cdot 10^{-13}$ m^2s^{-1}, respectively. The spray dried amorphous diffusivity found showed that there was sufficient time for the lactose to reach equilibrium in the sample pans.

The crystallisation of amorphous lactose was found to be all or nothing. With a variable $T-T_g$ the experimental data crystallised at a $T-T_g$ of 33.4°C compared with the 38°C predicted by the WLF equation. The Avrami-Bronlund model prediction of a gradual decrease in amorphicity was not followed. With a constant $T-T_g$ there was more data between the extremes, but the data was still mainly fully amorphous or showed no evidence of amorphicity. At a $T-T_g$ of 23.3°C pans began to show no evidence of amorphicity around 15.5 and 16.5 hours. The results reinforced the view that crystallisation is rapid. Two mechanisms for the rapid crystallisation, an auto catalytic effect and a showering event were proposed.

Results using partially amorphous lactose, Supertab, showed that crystallisation occurred at lower $T-T_g$ values than with regular amorphous lactose. At a $T-T_g$ of 23.3°C, there was no evidence of amorphicity after only 1.6 hours. The results suggest a seeding effect, giving some evidence for the showering event mechanism proposed to explain the rapid crystallisation.

6.1 Suggestions for future work

Given the difficulty in obtaining results between the states of completely amorphous and crystalline lactose a different method may be appropriate to elucidate further data. As well as the methods discussed in chapter 2, the idea of using a thin film of amorphous lactose and growing crystals could be investigated. This could be done using a polarised microscope allowing the crystallisation to be visually tracked. This has the advantage of isolating nucleation from crystal growth.

The method given to determine diffusivity can be used for a variety of different lactose or powder types. The DVS crystallisation method used could be used to find the minimum humidity required for crystallisation of amorphous lactose.

7 References

Aguilera, J. M., del Valle, J. M., & Karel, M. (1995). Caking phenomena in amorphous food powders. *Trends in Food Science and Technology, 6*, 149 - 155.

Bergqvist, A., & Soderqvist, J. (1999). *Characterisation of moisture induced crystallisation of lactose by isothermal calorimetry.* Degree Project - Chemical Engineering, Dalarna University, Borlange.

Bhandari, B. R., & Howes, T. (1999). Implication of glass transition for the drying and stability of dried foods. *Journal of Food Engineering, 40*(1-2), 71-79.

Billings, S. (2002). *The mathematical modelling of caking in bulk sucrose.* M.Eng., Massey University, Palmerston North, New Zealand.

Briggner, L.-E., Buckton, G., Bystrom, K., & Darcy, P. (1994). The use of isothermal microcalorimetry in the study of changes in crystallinity induced during the processing of powders. *International Journal of Pharmaceutics, 105*(2), 125-135.

Bronlund, J. E. (1997). *The modelling of caking in bulk lactose.* Ph.D., Massey University, Palmerston North, New Zealand.

Bronlund, J. E., & Paterson, A. H. J. (2004). Moisture sorption isotherms for crystalline, amorphous and predominately crystalline lactose powders. *International Dairy Journal, 14*, 247-254.

Brooks, G. F. (2000). *The sticking and crystallisation of amorphous lactose.* M.E., Massey University, Palmerston North, New Zealand.

Buckton, G., & Darcy, P. (1995). The influence of additives on the recrystallisation of amorphous spray dried lactose. *International Journal of Pharmaceutics, 121*, 81-87.

Buckton, G., & Darcy, P. (1996). Water mobility in amorphous lactose below and close to the glass transition temperature. *International Journal of Pharmaceutics, 136*, 141-146.

Buckton, G., Darcy, P., Greenleaf, D., & Holbrook, P. (1995). The use of isothermal microcalorimetry in the study of changes in crystallinity of spray-dried salbutamol sulphate. *International Journal of Pharmaceuticals, 116*, 113-118.

Buckton, G., Darcy, P., & Mackellar, A. J. (1995). The use of isothermal microcalorimetry in the study of small degrees of amorphous content of powders. *International Journal of Pharmaceutics*.

Burnett, D. J., Thielmann, F., Sokoloski, T., & Brum, J. (2006). Investigating the moisture-induced crystallization kinetics of spray-dried lactose. *International Journal of Pharmaceutics, 313*(1-2), 23-28. doi: 10.1016/j.ijpharm.2006.01.012

Che, L., & Chen, X. D. (2010). A simple nongravimetric technique for measurement of convective drying kinetics of single droplets. *Drying Technology, 28*(1), 73-77. doi: 10.1080/07373930903430744

Chen, X., Bates, S., & Morris, K. R. (2001). Quantifying amorphous content of lactose using parallel beam X-ray powder diffraction and whole pattern fitting. *Journal of Pharmaceutical and Biomedical Analysis, 26*(1), 63-72. doi: 10.1016/s0731-7085(01)00346-6

Chiou, D., & Langrish, T. A. G. (2008). A comparison of crystallisation approaches in spray drying. *Journal of Food Engineering, 88*(2), 177-185. doi: 10.1016/j.jfoodeng.2008.02.004

Crank, J. (1956). *The mathematics of Diffusion*. Oxford: Clarendon Press.

Das, D., & Langrish, T. A. G. (2012). An activated-state model for the prediction of solid-phase crystallization growth kinetics in dried lactose particles. *Journal of Food Engineering, 109*(4), 691-700. doi: 10.1016/j.jfoodeng.2011.11.024

Downton, G. E., Flores-Luna, J. L., & King, C. J. (1982). Mechanism of stickiness in hygroscopic, amorphous powders. *Industrial and Engineering Chemistry Fundamentals, 21*, 447-451.

Elmonsef Omar, A. M., & Roos, Y. H. (2007). Glass transition and crystallization behaviour of freeze-dried lactose-salt mixtures. *LWT - Food Science and Technology, 40*(3), 536-543. doi: 10.1016/j.lwt.2005.12.007

Feral, P. (2010). *The influence of lactic acid on the glass transition temperature of spray-dried and freeze-dried lactose powders.* Internship Report, Massey University, Palmerston North.

Figura, L. O., & Epple, M. (1995). Anhydrous [alpha]-lactose: A study with DSC and TXRD. *Journal of Thermal Analysis, 44*, 45-53.

Fix, I., & Steffens, K. J. (2004). Quantifying low amorphous or crystalline amounts of alpha-lactose- monohydrate using X-ray powder diffraction, near-infrared spectroscopy, and differential scanning calorimetry. *Drug Development and Industrial Pharmacy, 30*(5), 513-523. doi: 10.1081/ddc-120037482

Fu, N., Woo, M. W., Moo, F. T., & Chen, X. D. (2012). Microcrystallization of lactose during droplet drying and its effect on the property of the dried particle. *Chemical Engineering Research and Design, 90*(1), 138-149.

Gabbott, P., Clarke, P., Mann, T., Royall, P., & Shergill, S. (2003). A high-sensitivity, high-speed DSC technique: Measurement of amorphous lactose. *American Laboratory, 35*(16), 17-22.

Gombás, Á., Szabó-Révész, P., Kata, M., Regdon Jr, G., & Eros, I. (2002). Quantitative determination of crystallinity of α-lactose monohydrate by DSC. *Journal of Thermal Analysis and Calorimetry, 68*(2), 503-510. doi: 10.1023/a:1016039819247

Gordon, M., & Taylor, J. S. (1952). Ideal copolymers and the second-order transitions of synthetic rubbers. I. Non-crystalline copolymers. *Journal of Applied Chemistry, 2*, 493-500.

Greenspan, L. (1977). Humidity fixed points of binary saturated aqueous solutions. *Journal of research of the national bureau of standards - A. Physics and Chemistry, 81A*(1), 89-96.

Gustafsson, C., Lennholm, H., Iversen, T., & Nyström, C. (1998). Comparison of solid-state NMR and isothermal microcalorimetry in the assessment of the amorphous component of lactose. *International Journal of Pharmaceutics, 174*(1-2), 243-252. doi: 10.1016/s0378-5173(98)00272-5

Haque, M. K., & Roos, Y. H. (2004). Water Plasticization and Crystallization of Lactose in Spray-dried Lactose/Protein Mixtures. *Journal of Food Science, 69*(1), FEP23-FEP29. doi: doi:10.1111/j.1365-2621.2004.tb17863.x

Haque, M. K., & Roos, Y. H. (2006). Differences in the physical state and thermal behavior of spray-dried and freeze-dried lactose and lactose/protein mixtures. *Innovative Food Science & Emerging Technologies, 7*(1-2), 62-73.

Hardy, B. (1998). *ITS-90 Formulations for vapor pressure, frostpoint temperature, dewpoint temperature, and enhancement factors in the range -100 to +100 C.* Paper presented at the The Proceedings of the Third International Symposium on Humidity & Moisture, Teddington, London, England, April 1998.

Harjunen, P., Lehto, V. P., Koivisto, M., Levonen, E., Paronen, P., & Järvinen, K. (2004). Determination of amorphous content of lactose samples by solution calorimetry. *Drug Development and Industrial Pharmacy, 30*(8), 809-815. doi: 10.1081/ddc-200030302

Harper, W. J. (1992). Lactose and lactose derivatives. In J. G. Zadow (Ed.), *Whey and lactose processing* (pp. 317-360). Essex, England: Elsevier Applied Science.

Hogan, S. A., & O'Callaghan, D. J. (2010). Influence of milk proteins on the development of lactose-induced stickiness in dairy powders. *International Dairy Journal, 20*(3), 212-221. doi: 10.1016/j.idairyj.2009.11.002

Hogan, S. E., & Buckton, G. (2000). The quantification of small degrees of disorder in lactose using solution calorimetry. *International Journal of Pharmaceutics, 207*(1-2), 57-64. doi: 10.1016/s0378-5173(00)00527-5

Hogan, S. E., & Buckton, G. (2001). The Application of Near Infrared Spectroscopy and Dynamic Vapor Sorbtion to Quantify Low Amorphous Contents of Crystalline Lactose. *Pharmaceutical Research, 18*(1), 112-116.

Ibach, A., & Kind, M. (2007). Crystallization kinetics of amorphous lactose, whey-permeate and whey powders. *Carbohydrate Research, 342*(10), 1357-1365.

Kedward, C. J., MacNaughtan, W., & Mitchell, J. R. (2000). Crystallization Kinetics of Amorphous Lactose as a Function of Moisture Content Using Isothermal Differential Scanning Calorimetry. *Journal of Food Science, 65*(2), 324-328. doi: doi:10.1111/j.1365-2621.2000.tb16001.x

Kellam, S. (1998). The manufacture of lactose. *The Dairy Industry*. Retrieved 29 August, 2007, from http://www.nzic.org.nz/ChemProcesses/dairy/3F.pdf

Kirk, J. H., Dann, S. E., & Blatchford, C. G. (2007). Lactose: A definitive guide to polymorph determination. *International Journal of Pharmaceutics*(334), 103-114.

Langrish, T. A. G. (2008). Assessing the rate of solid-phase crystallization for lactose: The effect of the difference between material and glass-transition temperatures. *Food Research International, 41*(6), 630-636. doi: 10.1016/j.foodres.2008.04.010

Langrish, T. A. G., & Wang, S. (2009). Crystallization rates for amorphous sucrose and lactose powders from spray drying: A comparison. *Drying Technology, 27*(4), 606-614. doi: 10.1080/07373930802716391

Lehto, V. P., Tenho, M., Vaha-Heikkila, K., Harjunen, P., Paallysaho, M., Valisaari, J., . . . Jarvinen, K. (2006). The comparison of seven different methods to quantify the amorphous content of spray dried lactose. *Powder Technology*, 85-93.

Levine, H., & Slade, L. (1986). A polymer physicochemical approach to the study of commercial starch hydrolysis products (SHP's). *Carbohydr. Polym., 6*, 213-244.

Lin, S. X. Q., & Chen, X. D. (2002). Improving the glass-filament method for accurate measurement of drying kinetics of liquid droplets. *Chemical Engineering Research and Design, 80*(4), 400-409.

Lin, S. X. Q., & Chen, X. D. (2006). A model for drying of an aqueous lactose droplet using the reaction engineering approach. *Drying Technology, 24*(11), 1329-1334. doi: 10.1080/07373930600951091

Listiohadi, Y., Hourigan, J. A., Sleigh, R. W., & Steele, R. J. (2008). Moisture sorption, compressibility and caking of lactose polymorphs. *International Journal of Pharmaceutics, 359*(1-2), 123-134. doi: 10.1016/j.ijpharm.2008.03.044

Listiohadi, Y., Hourigan, J. A., Sleigh, R. W., & Steele, R. J. (2009). Thermal analysis of amorphous lactose and σ-lactose monohydrate. *Dairy Science and Technology, 89*(1), 43-67. doi: 10.1051/dst:2008027

Lloyd, R. J., Chen, X. D., & Hargreaves, J. B. (1996). Glass transition and caking of spray-dried lactose. *International Journal of Food Science and Technology, 31*(4), 305-311.

Mackin, L., Zanon, R., Min Park, J., Foster, K., Opalenik, H., & Demonte, M. (2002). Quantification of low levels (<10%) of amorphous content in micronised active batches using dynamic vapour sorption and isothermal microcalorimetry. *International Journal of Pharmaceuticals, 231*, 227-236.

McLeod, J. (2007). *Nucleation and growth of alpha lactose monohydrate.* PhD, Massey University, Palmerston North, New Zealand.

Miao, S., & Roos, Y. H. (2005). Crystallization kinetics and X-ray diffraction of crystals formed in amorphous lactose, trehalose, and lactose/trehalose mixtures. *Journal of Food Science, 70*(5), E350-E358.

Newell, H. E., Buckton, G., Butler, D. A., Thielmann, F., & Williams, D. R. (2001). The use of inverse phase gas chromatography to measure the surface energy of crystalline, amorphous, and recently milled lactose. *Pharmaceutical Research, 18*(5), 662-666. doi: 10.1023/a:1011089511959

Nijdam, J., Ibach, A., Eichhorn, K., & Kind, M. (2007). An X-ray diffraction analysis of crystallised whey and whey-permeate powders. *Carbohydrate Research, 342*(16), 2354-2364. doi: 10.1016/j.carres.2007.08.001

Nijdam, J., Ibach, A., & Kind, M. (2008). Fluidisation of whey powders above the glass-transition temperature. *Powder Technology, 187*(1), 53-61. doi: 10.1016/j.powtec.2008.01.013

Palzer, S. (2005). The effect of glass transition on the desired and undesired agglomeration of amorphous food powders. *Chemical Engineering Science, 60*(14), 3959-3968.

Palzer, S. (2010). The relation between material properties and supra-molecular structure of water-soluble food solids. *Trends in Food Science & Technology, 21*(1), 12-25.

Paterson, A. H. J. (2009). Production and uses of lactose. In P. F. Fox & P.L.H.McSweeney (Eds.), *Advanced Dairy Chemistry* (Vol. 3, pp. 105-121). New York: Springer Science+Business Media, LLC.

Paterson, A. H. J. (2012). *Spray Drier Mass balance*. Massey University.

Paterson, A. H. J., Brooks, G. F., Foster, K. D., & Bronlund, J. E. (2005). The development of stickiness in amorphous lactose at constant T−Tg levels. *International Dairy Journal, 15*, 513-519.

Ripberger, G. (2010). *Mechanism of viscous droplet/solid stickiness during impact investigation of the diffusivity and viscosity of amorphous lactose.* German Diploma Thesis, Massey University, Palmerston North.

Roelfsema, W. A., Kuster, B. F. M., Heslinga, M. C., Pluim, H., & Verhage, M. (2000). *Lactose and Derivatives*: Wiley-VCH Verlag GmbH & Co. KGaA.

Roetman, K., & Buma, T. J. (1974). Temperature dependence of the equilibrium β/α ratio of lactose in aqueous solution. *Netherlands Milk and Dairy Journal, 28*, 155-165.

Roos, Y., & Karel, M. (1990). Differential scanning calorimetry study of the phase transitions affecting the quality of dehydrated materials. *Biotechnology Progress, 6*, 159-163.

Roos, Y., & Karel, M. (1991). Plasticizing effect of water on thermal behavior and crystallization of amorphous food models. *Journal of Food Science, 56*(1), 38-43.

Roos, Y., & Karel, M. (1992). Crystallization of Amorphous Lactose. *Journal of Food Science, 57*(3), 775-777.

Saunders, M., Podluii, K., Shergill, S., Buckton, G., & Royall, P. (2004). The potential of high speed DSC (Hyper-DSC) for the detection and quantification of small amounts of amorphous content in predominantly crystalline samples. *International Journal of Pharmaceutics, 274*(1-2), 35-40. doi: 10.1016/j.ijpharm.2004.01.018

Schmitt, E. A., Law, D., & Zhang, G. G. Z. (1999). Nucleation and Crystallization Kinetics of Hydrated Amorphous Lactose above the Glass Transition Temperature. *Journal of Pharmaceutical Sciences, 88*(3), 291-296.

Sebhatu, T., Angberg, M., & Ahlneck, C. (1994). Assessment of the Degree of Disorder in Crystalline Solids by Isothermal Microcalorimetry. *International Journal of Pharmaceutics, 104*, 165-144.

Shah, B., Kakumanu, V. K., & Bansal, A. K. (2006). Analytical techniques for quantification of amorphous/crystalline phases in pharmaceutical solids. *Journal of Pharmaceutical Sciences, 95*(8), 1641-1665. doi: 10.1002/jps.20644

Tang, X., & Pikal, M. J. (2004). Design of freeze-drying processes for pharmaceuticals: practical advice. *Pharmaceutical Research, 21*(2), 191-200.

Thomsen, M. K., Jespersen, L., Sjostrom, K., Risbo, J. R., & Skibsted, L. H. (2005). Water activity - temperature state diagram of amorphous lactose. *Journal of Agriculture and Food Chemistry, 53*, 9182-9185.

Timmermann, E. O., & Chirife, J. (1991). The physical state of water sorbed at high activities in starch in terms of the GAB sorption equation. *Journal of Food Engineering, 13*, 171-179.

Tsourouflis, S., Flink, J. M., & Karel, M. (1976). Loss of Structure in Freeze-Dried Carbohydrate Solutions: Effect of Temperature, Moisture Content and Composition. *Journal of the Science of Food and Agriculture, 27*, 509-519.

Vivoda, M., Roškar, R., & Kmetec, V. (2011). The development of a quick method for amorphicity determination by isothermal microcalorimetry. *Journal of Thermal Analysis and Calorimetry, 105*(3), 1023-1030.

Vollenbroek, J., Hebbink, G. A., Ziffels, S., & Steckel, H. (2010). Determination of low levels of amorphous content in inhalation grade lactose by moisture sorption isotherms. *International Journal of Pharmaceutics, 395*(1-2), 62-70.

Vuataz, G. (1988). Preservatin of Skim-Milk Powders : Role of Water Activity and Temperature in Lactose Crystallization and Lysine Loss. In C. C. Seow (Ed.), *Food Preservation by Moisture Content* (pp. 73-101). New York: Elsevier Applied Science.

Vuataz, G. (2002). The phase diagram of milk: a new tool for optimising the drying process. *Lait, 82*, 485-500.

Whiteside, P. T., Luk, S. Y., Madden-Smith, C. E., Turner, P., Patel, N., & George, M. W. (2008). Detection of low levels of amorphous lactose using H/D exchange and FT-Raman spectroscopy. *Pharmaceutical Research, 25*(11), 2650-2656. doi: 10.1007/s11095-008-9682-4

Williams, M. L., Landel, R. F., & Ferry, J. D. (1955). The temperature dependence of relaxation mechanisms in amorphous polymers and other glass-forming liquids. *Journal of the American Chemical Society, 77*, 3701-3707.

Yazdanpanah, N., & Langrish, T. (2011). Fast crystallization of lactose and milk powder in fluidized bed dryer/crystallizer. *Dairy Science & Technology, 91*(3), 323-340. doi: 10.1007/s13594-011-0015-8

8 Appendices

8.1 Sensor data

8.1.1 RH heating peak

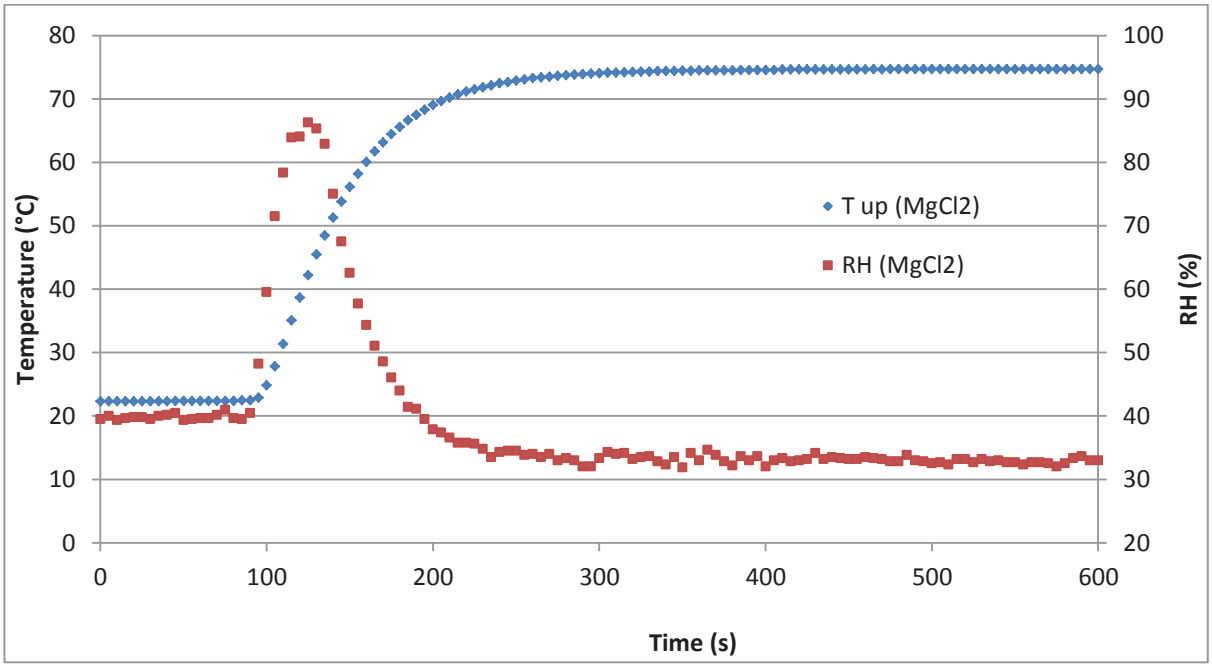

Figure 8-1: RH peak displayed by ibuttons during heating.

8.1.2 Heating and cooling rates

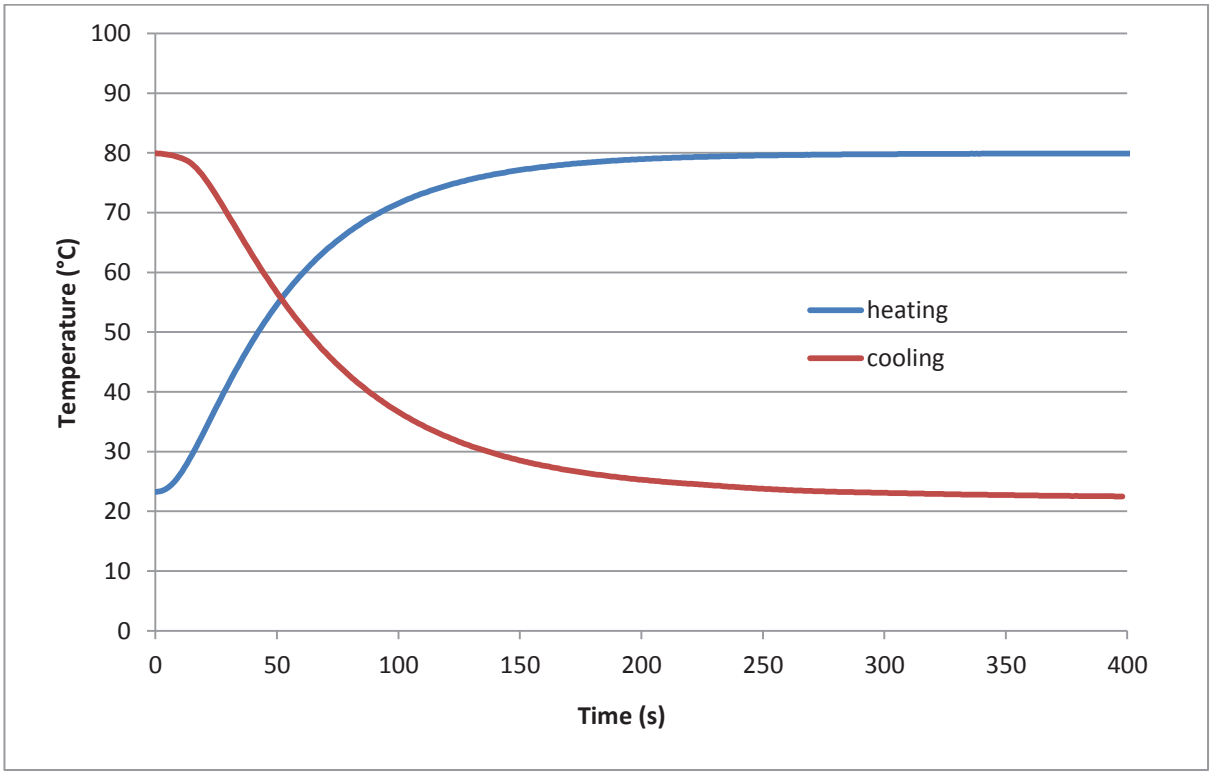

Figure 8-2: Heating and cooling rate of sample pan using ibutton data.

8.2 XRD data

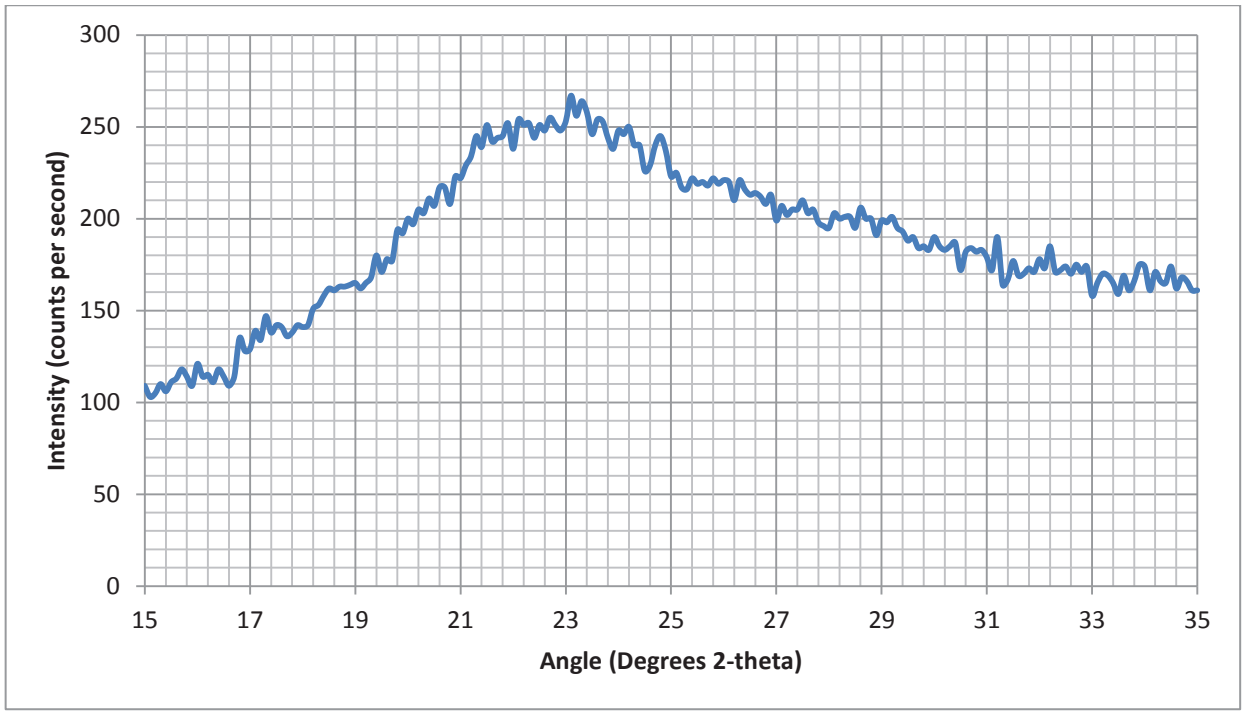

Figure 8-3: XRD data for spray dried amorphous lactose produced using GEA niro spray dryer. Analysed in 2θ range from 15° to 35° at a speed of 0.1 °/min.

8.3 Code for User Defined Functions

8.3.1 Diffusion Total

```
Public Function diffYtot(Fo As Double) As Double

   'Uses Crank 1956 analytical solution for unsteady state diffusion into a sphere

   'Returns total amount of diffusing substance into or out of sphere from Fourier number


   Dim a As Double

Dim x As Double

   Dim iAs Long


a = 0


   For i = 1 To 100


      x = (1 / i ^ 2) * Exp(-(i ^ 2) * Application.WorksheetFunction.Pi() ^ 2 * Fo)


      a = a + x


      If Abs(x) < 1 * 10 ^ (-15) Then          'If new term is very small then finish summation

         Exit For

      End If


   Next


diffYtot = 1 - 6 / Application.WorksheetFunction.Pi() ^ 2 * a

End Function
```

8.3.2 Diffusion Total with Particle Size Distribution

```
Public Function diffYtotpz(t As Double, D As Double, ParamArraySizeClass() As Variant) As
Double

   'Takes Nx2 array of particle size (um) by volume fraction (%) and calculates accomplished
change for each by calling diffYtot

   'Ytotpz is then the sum of volume fraction multiplied by accomplished change for each
particle size


   Dim SizeClasstempAs Variant

   Dim j As Long

   Dim R As Double

Dim Fo As Double

Dim Y As Double

   Dim YtotAs Double


SizeClasstemp = SizeClass(0).Value


   For j = LBound(SizeClasstemp) To UBound(SizeClasstemp)


      R = SizeClasstemp(j, 1) * 0.5                    'Radius


Fo = t * 60 * D / (R / 10 ^ 6) ^ 2            'Fourier number

       Y = diffYtot(Fo)                                 'Calls diffYtot for particle size R

Ytot = Y * SizeClasstemp(j, 2) / 100 + Ytot     'Sums by volume fraction


   Next


diffYtotpz = Ytot

End Function
```